AD NUMBER

AD881534

NEW LIMITATION CHANGE

TO

Approved for public release, distribution unlimited

FROM

Distribution authorized to U.S. Gov't. agencies only; Administrative/Operational Use; JAN 1971. Other requests shall be referred to Air Force Weapons Laboratory, Attn: SRR, Kirtland AFB, NM 87117.
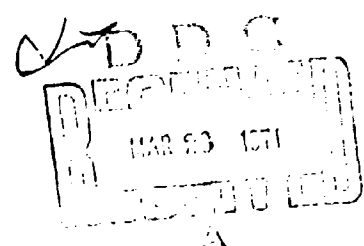
AUTHORITY

AFWL ltr, 17 Apr 1974

AD881534

DYNAMIC FRACTURE IN
6061-T6 ALUMINUM

James R. Kreer
Capt   USAF

TECHNICAL REPORT NO. AFWL-TR-70-180

January 1971

AIR FORCE WEAPONS LABORATORY
Air Force Systems Command
Kirtland Air Force Base
New Mexico

73

DYNAMIC FRACTURE IN 6061-T6 ALUMINUM

James R. Kreer
Capt   USAF

TECHNICAL REPORT NO. AFWL-TR-70-180

AFWL-TR-70-180

AIR FORCE WEAPONS LABORATORY
Air Force Systems Command
Kirtland Air Force Base
New Mexico   87117

FOREWORD

This research was performed under Program Element 61102H, Project 5710, Subtask AA 114, and was funded by the Defense Atomic Support Agency (DASA).

Inclusive dates of research were June 1969 through October 1970. The report was submitted 16 December 1970 by the Air Force Weapons Laboratory Project Officer, Captain James R. Kreer (SRR).
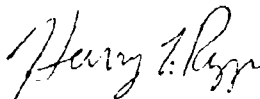
This technical report has been reviewed and is approved.

James R Kreer

JAMES R. KREER
Captain, USAF
Project Officer

Durward D. Young, Jr

DURWARD D. YOUNG, JR.
Lt Colonel, USAF
Chief, Radiation Effects Branch

Harry F Rizzo

HARRY F. RIZZO
Lt Colonel, USAF
Chief, Radiation Division

ABSTRACT

(Distribution Limitation Statement No. 3)

Gas gun impact experiments were performed on five thicknesses of 6061-T6 aluminum targets to determine the incipient spall threshold. Data obtained were compared with previous data for the same material obtained by General Motors and other laboratories. Results indicated that batch-to-batch variations in properties of a commercially "standard" material may cause up to 15 percent differences in spall thresholds for short duration (<0.1 μ second) shock loads. Four mathematical models of dynamic fracture were evaluated with the spall data obtained. The Hole-Growth model developed by Stanford Research Institu.e under contract to the Air Force Weapons Laboratory proved superior to the other models considered. This superiority was manifested in the ease of interpretation of the calculated damage levels and the physical significance of the calculations.

CONTENTS

ILLUSTRATIONS

ILLUSTRATIONS (cont'd)

TABLES

SECTION I

INTRODUCTION

Studies of dynamic failure in homogeneous materials have been of particular interest to the USAF and DOD because of the applicability of such studies to weapons systems subjected to a nuclear detonation. Absorption of a given dose of X rays by a weapons system causes a high-amplitude, short-duration, compressive shock pulse to propagate through weapon heat shields and metal substructures. This pulse is reflected from a free surface or interface as a relief wave propagating in the opposite direction. The interaction of relief waves causes tension in the material. The behavior of the material as a result of this tension is important because catastrophic failure or significant degradation of structural properties may result.

Many studies have been made of time-dependent fracture in homogeneous materials. One material which has undergone extensive investigation is 6061-T6 aluminum because its behavior under dynamic loading conditions appears to be relatively strain-rate insensitive (figure 1). The Air Force Weapons Laboratory (AFWL) undertook a study of 6061-T6 aluminum to determine its spallation threshold. This report provides a description of the experimental technique, a summary of the results obtained, a comparison of those results with data obtained by other laboratories, and an evaluation of a few of the mathematical models of dynamic fracture currently available.
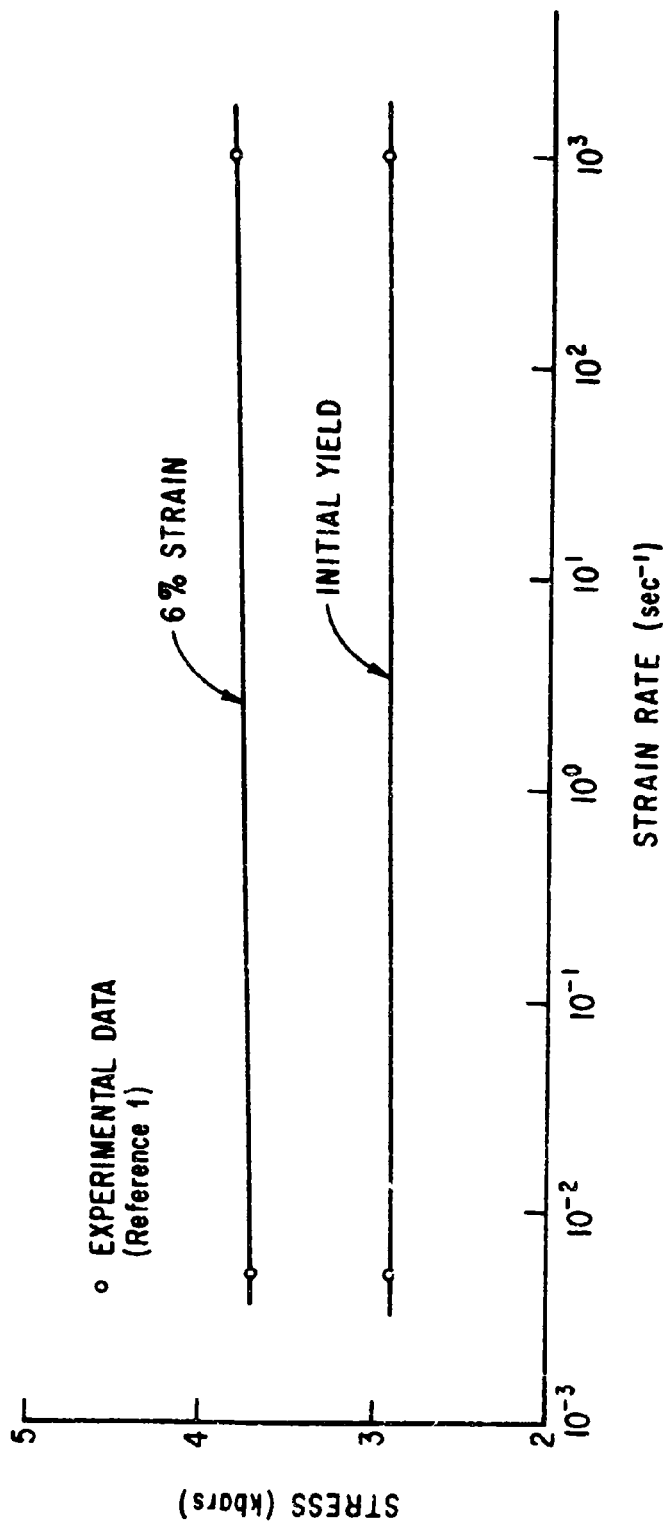
Figure 1. Strain Rate Sensitivity of 6061-T6 Aluminum at Room Temperature

SECTION II

EXPERIMENTAL TECHNIQUE

As mentioned in section I, absorption of X rays by a material gives rise to
a compressive pulse of high amplitude and short duration which reflects from free
surfaces or material interfaces to produce tension. In the homogeneous materials
such as metals, this tension results in the nucleation of microcracks or voids
and their subsequent growth. When the tensile stress reaches still higher ampli-
tudes or longer durations, these cracks begin to coalesce and total separation
of the material can occur.

Simualtion techniques exist through which compressive shock waves similar to
those caused by X-ray deposition can be introduced into a material. One such
technique is the high-velocity impact on a target material by a flyer plate.
This was the method chosen for the study being reported. A schematic drawing of
the experimental apparatus is shown in figure 2. The flyer plate is accelerated
by a sabot to its impact velocity which is measured by three velocity pins. After
the flyer plate impacts the target, the sabot is stopped. Both target and flyer
are recovered from a catching mechanism.

Figure 3 shows a cross-sectional view of both the target and flyer plates.
All plates were machined from 1/4 inch thick plate stock. The ratio of target
thickness to flyer thickness was kept at the constant value of 7:1. There were
two reasons for the choice of this ratio. First, making the target twice the
thickness of the flyer, and of the same material, forces the duration of the shock
pulse to be approximately equal to the transit time of the shock across the tar-
get and thereby minimizes attenuation of the pulse due to the trailing rarefaction
wave. The choice of this ratio also causes spallation to occur at approximately
the midplane of the target. The first interaction of two rarefaction waves and,

3
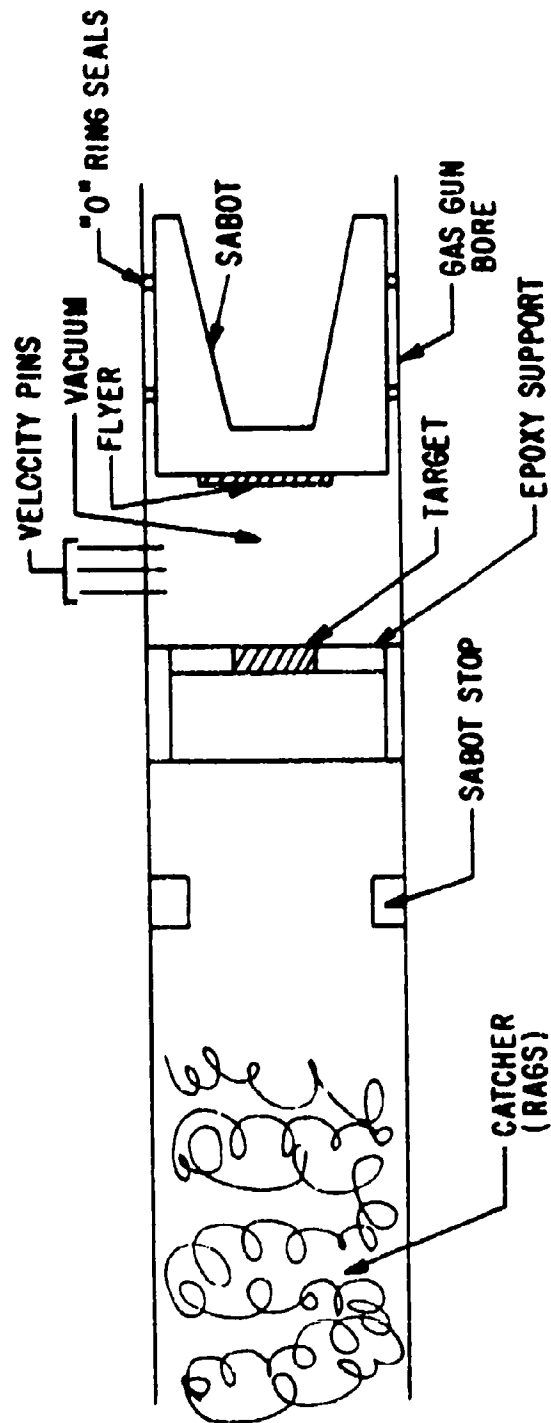
Figure 2.   Schematic Drawing of Experimental Apparatus

4
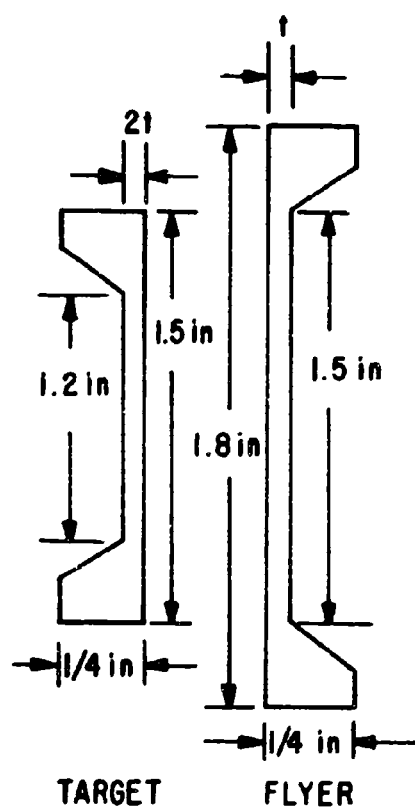
Figure 3. Target Plate Cross Section
and Flyer Plate Cross Section

5

thus, the first tensile stress, occurs at this plane. The simple X-t curve shown in figure 4 demonstrates both of these points and also shows that the midplane of the target is under tensile stress for the longest period of time. herefore, the microcracks that form in the target material are concentrated around this plane.

Previous experimenters had demonstrated the time-dependency of spall in homogeneous materials (Ref 1-6). The objective of this experiment was to determine the threshold for incipient spall in 6061-T6 aluminum. For purposes of the experiment, incipient spall is defined as the amount of damage that occurs such that the spall plane is 50 percent covered by voids or cracks. The spall plane is the plane which is under tension for the longest period of time.

In impact experiments such as these, the duration of the pulse varies with the thickness of the flyer, while the amplitude of the pulse is proportional to the impact velocity. For the original experiment, five different flyer thicknesses were chosen such that the pulse durations would vary from less than 0.1 μsec to greater than 0.5 μsec. There would be five flyers of each thickness fired at a range of velocities both above and below the critical velocity for incipient spall for that thickness. The end result was to be five data points on the incipient spall threshold for 6061-T6 aluminum.

To determine the degree of damage, the following technique was employed: Each target was recovered from the catcher mechanism at the completion of the shot. Abnormalities such as off-center impact or indications of multiple impacts were noted at this time. The samples were sectioned, mounted, and polished. Each sample was then examined for damag. _. magnifications of both 50X and 100X, and photomicrographs were taken. The results of the program are presented in section III.
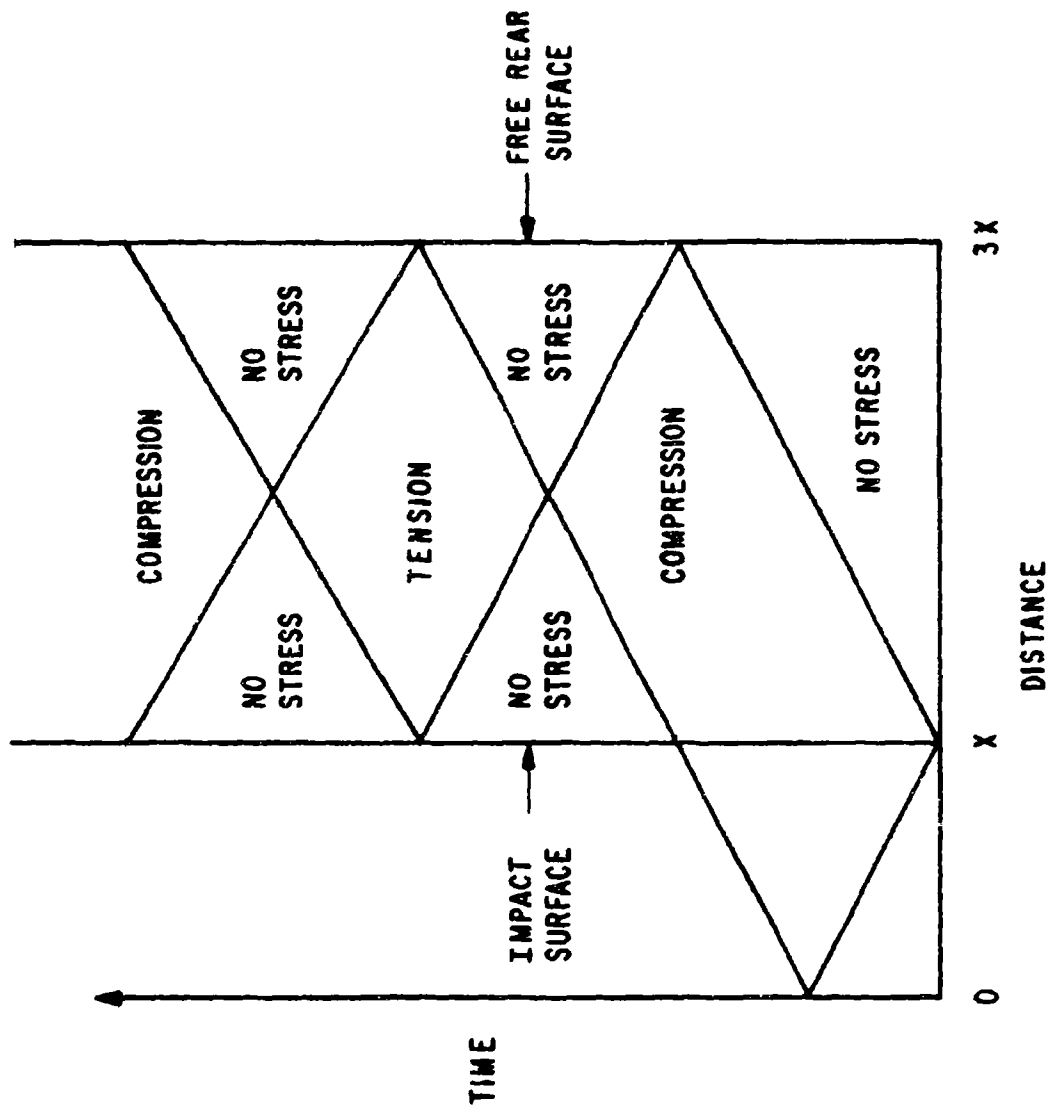
Figure 4. Simple x-t Diagram for 6061-T6 Aluminum

7

SECTION III

EXPERIMENTAL RESULTS

Each of the recovered target specimens was examined for damage and each was classified according to figure 5 on the following page. The results of the first 25 gas-gun shots are tabulated and illustrated in figure 6.

Figure 6 shows the time-dependence of the spall phenomenon. Those specimens which undergo tensile stress through a longer time duration begin to fracture at somewhat lower stress levels than those which are under tension for a shorter period of time.

This first series of gas-gun shots indicated some problems with the experimental configuration. Note in table I that with the thinnest targets no spall was detected at all. However, with the 32-mil targets, some damage was present with even the lowest velocity flyer. The steep rise in spall threshold indicated in figure 6 for the thinnest flyers (shortest pulse durations) was not expected and did not compare at all to previous data obtained for the same material. Most notably, General Motors, in work performed under the DASA-sponsored PREDIX program, had reported damage in 20-mil targets from 10-mil flyers with a velocity of approximately 860 ft/sec (Ref 1).

Since the experimental technique used by both AFWL and GM was practically identical, a reasonable explanation was sought for this discrepancy. It is known that the gas-gun impact technique provides a very flat impact. Planarity did not appear to be the problem. Timing devices had recently been calibrated, and measured velocities were accurate to ±2 percent.

It was then noted that all of the specimens had some surface curvature and that this effect seemed to be more pronounced in the thinner targets. It was possible that, at the high velocities being used, the thin flyers were bowing

8
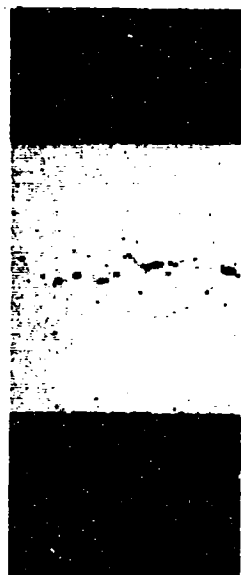
Figure 5. Levels of Damage in Spalled Target Specimens

9
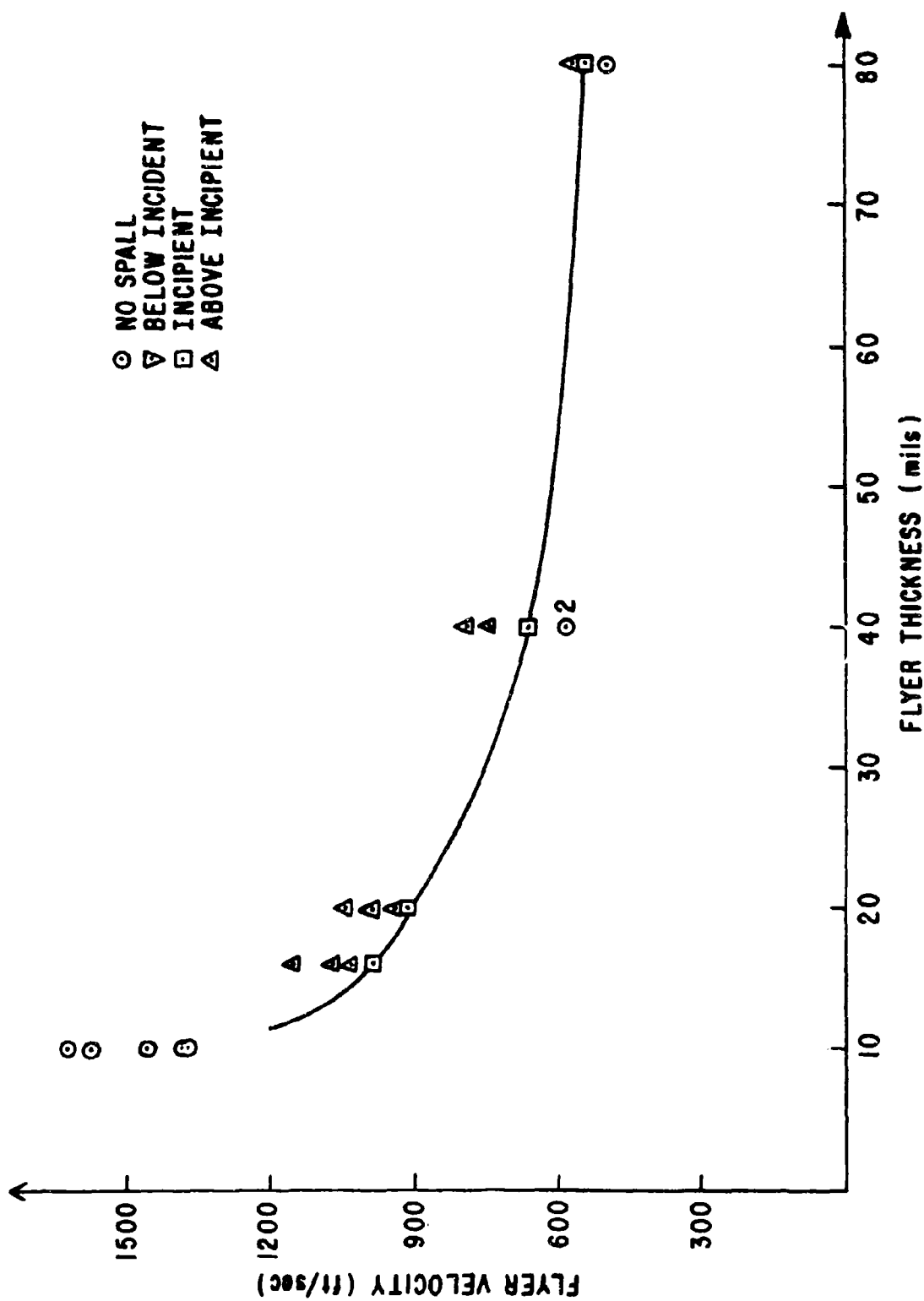
Figure 6. Results of Series I Impacts

Table I

RESULTS OF SERIES I IMPACTS

Flyer Thickness (mils)	Target Thickness (mils)	Velocity (ft/sec)	Results
10	20	1373	No spall
		1383	No spall
		1455	No spall
		1571	No spall
		1619	No spall
16	32	850	Not fired
		983	Incipient
		1028	Above incipient
		1064	Above incipient
		1150	Above incipient
20	40	864	Not recovered
		913	Incipient
		938	Above incipient
		985	Above incipient
		1040	Above incipient
40	80	575	No spall
		581	No spall
		661	Incipient
		744	Above incipient
		790	Above incipient
80	160	450	Not fired
		490	No spall
		534	Incipient
		560	Above Incipient
		650	Not fired

severely and the actual impact velocities in the center of the configuration were much less than those being measured. This would be the case if the flyer or target had to be deformed before impact occurred as this deformation would decelerate the flyer plate. Also, the thicker flyers with the same diameter would have greater stiffness, would bow less, and would provide more accurate results. Finally, the thin targets exhibited some spallation near the edges where the measured velocities were probably accurate, but no spallation in the center of the targets. For this experiment, only observations near the center of the targets were of interest. The results are to be used to validate models describing dynamic failure in homogeneous materials. These models would be incorporated into one dimensional, hydrodynamic computer codes such as the PUFF computer code. To observe failure which was primarily due to one-dimensional stress wave propagation, only the center region of the targets was of interest. Near the edges, two-dimensional effects arise due to shear waves reflected from the edges.

A second series of impact experiments was planned to examine the effects of bowing in the flyer plates. The results obtained for the 40-mil flyer impacts in series I compared favorably with incipient spall data for similar pulse durations obtained by other laboratories. Thus the diameter-to-thickness ratio for these flyers was adopted for the thinner flyers. At 40 mils, the ratio was

$$\frac{d_f}{x_f} = \frac{1.500}{0.040} = 37.5 \tag{1}$$

Using a ratio of 40:1 resulted in the diameters shown in table II.

The experimental matrix for series II included five shots for each flyer thickness, a total of fifteen shots. The velocities chosen were again varied so as to bracket the critical velocity for incipient spall for each flyer thickness. The results of this series are summarized in table III and illustrated in figure 7. Also shown for comparison in figure 7 are the General Motors data (Ref. 1). The agreement between the two sets of data is better although the AFWL curve

12

Table II

TARGET AND FLYER PLATE DIAMETERS FOR SERIES II IMPACTS

Flyer Thickness, x_f (mils)	Target Thickness, x_t (mils)	Flyer Diameter, d_f (in.)	Target Diameter, d_t (in.)
10	20	0.40	0.20
16	32	0.60	0.30
20	40	0.80	0.50

Table III

RESULTS OF SERIES II IMPACTS

Flyer Thickness (mils)	Target Thickness (mils)	Velocity (ft/sec)	Results
10	20	663	No spall
		726	No spall
		836	No spall
		970	Below incipient
16	32	1214	Above incipient
		650	No spall
		726	No spall
		843	Below incipient
		958	Incipient
		1188	Above incipient
20	40	690	No spall
		698	No spall
		853	Incipient
		956	Above incipient
		1025	Not fired

13
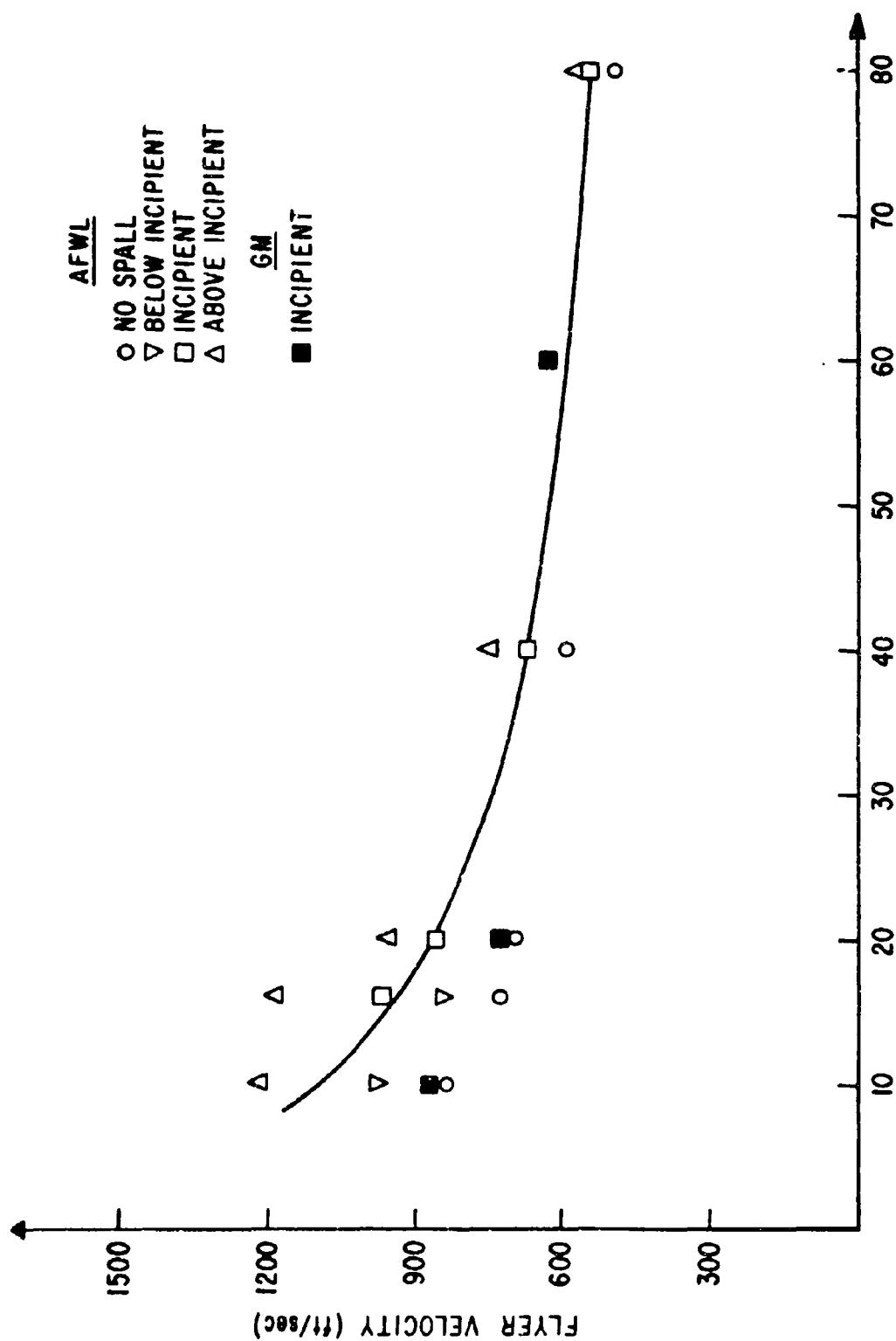
Figure 7. Comparison of AFWL and GM Spall Data

14

still exhibits a sharper rise (greater time dependence) for the thinnest flyers.

One final series of impact shots was planned to attempt to resolve the 25 percent difference in spall thresholds for short pulse durations. General Motors laboratory provided AFWL with some aluminum cut from the same plate which GM used for their spall experiments. The experimental configuration was identical to the AFWL shots, the only variable being the material. In this way it was hoped to determine   the spall threshold varied for the same material from batch to batch.

The experimental matrix chosen included four flyer thicknesses. For each thickness, two shots would be fired at the AFWL critical velocity and two shots at the GM critical velocity. The results of this series are summarized in table IV.

At best, these results are inconclusive. For all targets impacted at the AFWL critical velocities, resulting damage ranged from incipient to severe spall. At GM's critical velocities, the 20-mil targets showed some damage below the incipient level; while results for the 32-mil and 40-mil targets were ambiguous. However, closer examination of these shots does point out two interesting results.

In figure 8 the incipient spall thresholds determined by AFWL and by GM are plotted. The results of the series III impacts indicate a spall threshold occurring in the band created by previous data. In figures 9 and 10 damage resulting from impacts at nearly equal velocities in the AFWL aluminum and the GM aluminum is shown. It is obvious that in this commercially "standard" material, the GM aluminum was more severely damaged than the AFWL aluminum impacted at the same velocity.

Thus, one might conclude that difficulties encountered in attempts to duplicate spall data from laboratory to laboratory are complex enough without the added confusion contributed by variations in batch-to-batch qualities of

15

"standard" material. In addition, the spall threshold apparently is best defined by a band in which incipient spall will occur rather than a single curve.

Table IV

RESULTS OF SERIES III IMPACTS

Flyer Thickness (mils)	Target Thickness (mils)	Velocity (ft/sec)	Results
10	20	967	Below incipient
		982	Below incipient
		1089	Above incipient
		1108	Above incipient
16	32	841	No spall
		849	Incipient
		938	Incipient
		950	Above incipient
20	40	782	Incipient
		783	No spall
		857	Incipient
		864	Above incipient
40	80	627	Below incipient
		639	Incipient
		676	Above incipient
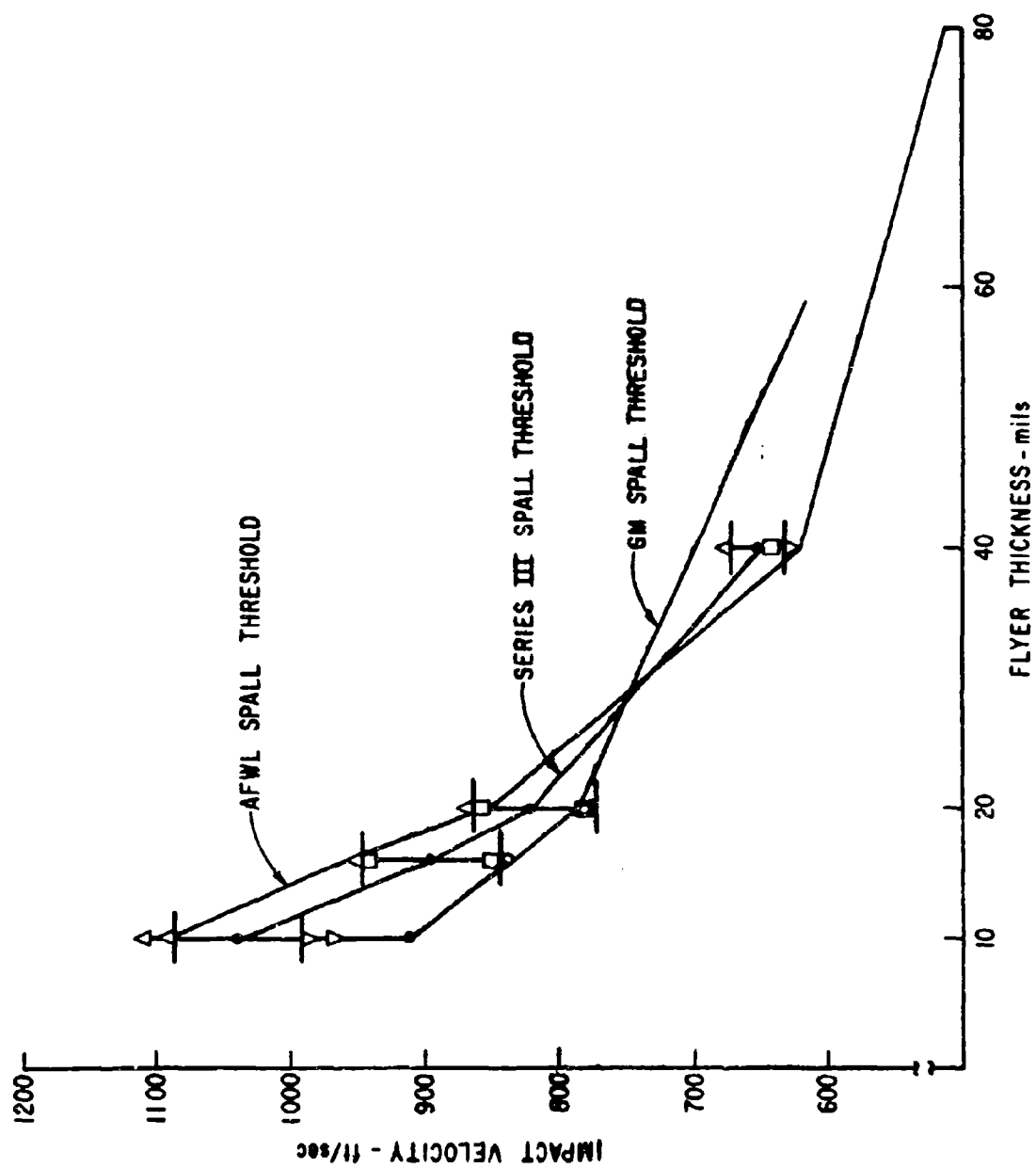
Figure 8. Series III Data Compared with AFWL and GM Spall Thresholds

AFWL   970 ft/sec

GM   967 ft/sec

NOT REPRODUCIBLE

GM   982 ft/sec

Figure 9.   Comparison of Damage in AFWL and GM Material
for 20 Mil Targets Impacted at Similar Velocities
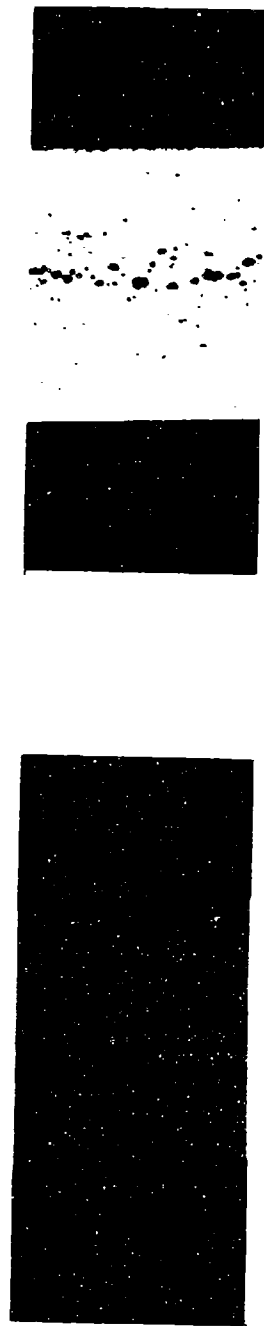
GM 849 ft/sec

GM 950 ft/sec

AFWL 843 ft/sec
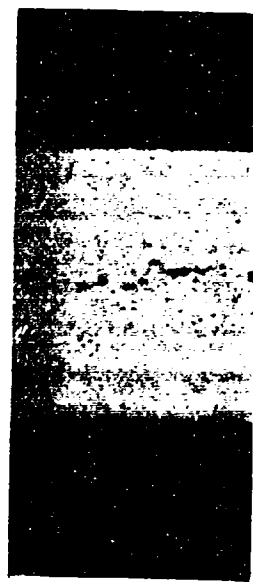
AFWL 958 ft/sec

Figure 10. Comparison of Damage in AFWL and GM Material
for 32 Mil Targets Impacted at Similar Velocities

SECTION IV

DATA ANALYSIS

The purpose of these experiments was to determine the time-dependent spall
threshold for 6061-T6 aluminum. These data were to be used to validate va1
dynamic fracture models proposed for inclusion in the PUFF computer code.
is a one-dimensional, Lagrangian, finite-difference code used to calculate the
response of layered homogeneous materials to high-amplitude, short-duration shock
loading. At present, the spall criterion used in the PUFF code is critical ten-
sile stress (Ref 7). This criterion is not valid for metals which, in general,
exhibit a time-dependency in their spall behavior. Thus, a dynamic spall criterion
would be a valuable addition to the PUFF code.

In this section, some of the dynamic fracture models considered by AFWL for
inclusion in the PUFF code will be discussed. These models will be compared with
AFWL experimental data as well as data obtained at other laboratories. Finally,
the results of including the models in the P-PUFF code (plate slap version of
PUFF) will be presented.

1. FRACTURE MODELS

A number of dynamic fracture models, both empirical and phenomenological,
have been developed in recent years. Those considered by AFWL for inclusion in
the PUFF code are summarized in table V. Other available models (Ref. 8-11) were
not included in this study because a similar model was studied, sufficient data
was not available for proper analysis, or the model was not easily adaptable to
the PUFF code.

The cumulative damage model was developed by Tuler and Butcher at Sandia
Laboratories. The constants are evaluated with experimental data for a given
material (Ref. 12). The term σ_o has been compared to both the static fracture

20

stress and the dynamic yield strength. The exponent λ can be assigned a value of 1.0 to correspond to an impulse criterion for failure, a value of 2.0 to correspond to an energy criterion, or some other value based on a best fit of experimental data. Generally, a value is assumed for either σ_o or λ and a least-squares analysis is used to solve for the other two constants. The cumulative damage model is independent of pulse shape since the integration can be solved for an arbitrary shape.

Table V

SUMMARY OF DYNAMIC FRACTURE MODELS

Model	Equation
1. Cumulative Damage	$\int_o^t (\sigma - \sigma_o)^\lambda \, dt = K$
2. Rate Process	$\sigma = A + B \log t$
3. Series Expansion	$\sigma = \sigma_o + \dfrac{A}{t} + \dfrac{B}{t}2 + \ldots$
4. Hole Growth	$R(t) = R_o \exp [A(\sigma)t]$

The rate process model of Cohen and Berkowitz (Ref. 13) requires the evaluation of only two constants, which can be done simply by a least-squares analysis. The difficulty with this model is the definition of the pulse duration t. For a perfectly rectangular pulse, the value is obvious. For an arbitrary pulse shape, the pulse duration is determined through consideration of impulse and a pulse shape constant k defined in reference 13.

The series expansion model was developed by the author for its mathematicl simplicity and the accuracy with which it reproduces experimental data. The model has no physical significance, but can use as many terms as necessary to obtain desired accuracy.

The Hole-Growth model was developed by Stanford Research Institute (SRI) under contract to AFWL. The model uses experimental impact data to determine the

21

nucleation rate and growth rate of voids or cracks as functions of stress ampli-
tude, stress duration, and instantaneous void size. Data for 1145 aluminum
indicate that the nucleation rate is constant and that the growth rate can be
described by the viscous flow relation

$$R(t) = R_o \exp [A(\sigma)t] \tag{2}$$

Where

$R(t)$ = void radius at time t

R_o = initial void radius

$A(\sigma)$ = growth parameter

Both of these functions are illustrated in figure 11. Stanford Research Insti-
tute has written two subroutines for the PUFF code which compute the initiation
and growth of voids in the material and the reduced tensile stress due to recom-
pression waves propagating outward from the newly formed free surfaces (Ref. 4).
Application of this model to the experimental data is limited because of the lack
of data on the fracture parameters for 6061-T6 aluminum. However, some PUFF runs
were made, and these are discussed in the final part of this section.

2. COMPARISON OF OBSERVED AND CALCULATED SPALL THRESHOLDS

To compare the AFWL incipient spall threshold data with the predictions of
the models and with data generated at other laboratories, the P-PUFF computer
code was used to convert the velocity-flyer thickness data to stress-time data.
The version of P-PUFF used is described in reference 14, and is basically an
elastic-plastic formulation using the Von Mises stress-dependent yield criterion.
The equation of state data used in the code calculations are provided in table VI.
Also shown for comparison in table VI is the equation of state data used by other
laboratories for 6061-T6 aluminum and data for mylar which are discussed later
in this section.

The PUFF code was run for each flyer thickness and the corresponding critical
velocity for incipient spall. The existing fracture routine was suppressed for

22

VOLUME OF VOIDS/INITIAL VOLUME OF MATERIAL

TIME (μsec)

NUMBER OF VOIDS/mm^3
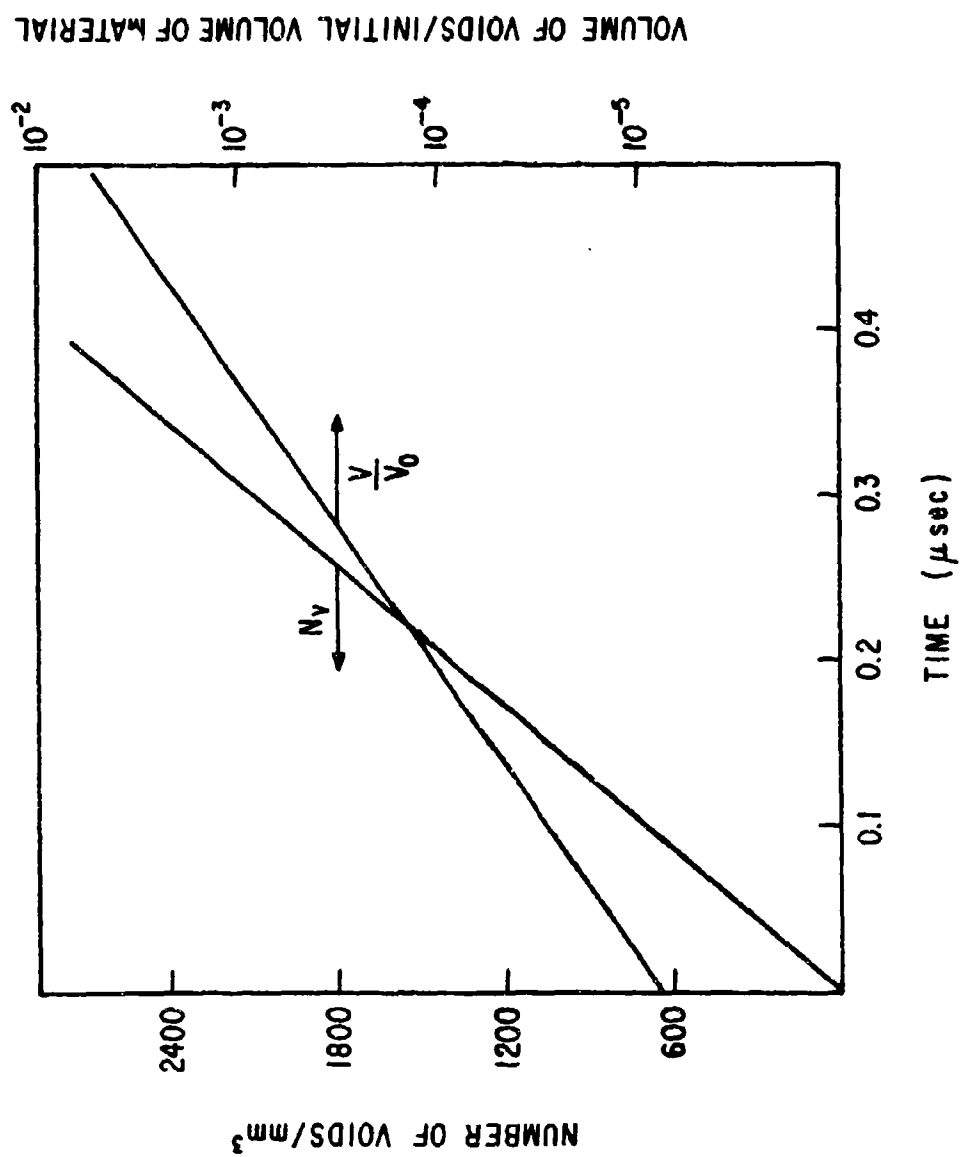
Figure 11. Void Density and Relative Void Volume vs. Time at Stress

Table VI

EQUATION OF STATE DATA FOR ALUMINUM AND MYLAR

Material	Reference	C(kb)	D(kb)	S(kb)	G	E_s(ergs/gm)	Yo(kb)	AMU(kb)	YMU	ρ(gm/cm^3)
6061-T6 Al	AFWL (15)	733.98	1859.73	-26982.35	2.03	1.1768×10^{11}	2.6995	275.16	0.0049	2.704
6061-T6 Al	S^3 (16)	720.0	1313.0	2008.0	2.13	1.2×10^{11}		277.0		2.70
6061-T6 Al	MDAC (17)	760.0	1293.0	816.0	2.13		2.53	205.7		2.70
6061-T6 Al	SLA (18)	768.0	844.2	-1338.0	2.13	0.3232×10^{11}	3.3	293.4		2.71
Mylar	AFWL (15)	67.28	145.49	236.27	1.00	0.44×10^{11}	0.0	0.0	0.0	1.39
Mylar	MDAC (17)	71.3	131.0	200.0	0.448	-	0.0	0.0	0.0	1.39

these runs. A plot of the stress-time history at the midplane of the target was obtained, a sample of which is shown in figure 12.

Using the printed code output and the stress-time histories for the AFWL equation of state, a peak tensile stress and pulse duration were determined for each flyer thickness, providing five data points on the stress-pulse duration spall threshold (fig. 13). The pulse duration was taken as the width of the pulse at 4.25 kilobars according to the convention established by the PREDIX group (Ref. 19). Other laboratories have used the width at peak stress, at zero stress, and at half maximum. Some convention is necessary since these histories are quasi-retangular and the pulse width may vary considerably from peak to zero stress. The value of 4.25 kilobars (the static yield limit) emerged from the PREDIX studies as the value of σ_0 in the Tuler-Butcher spall model, and pulse durations were taken at this stress level. The indicated error bars of approximately 10 percent in figure 13 are based upon increments in velocities and visual approximations of the level of damage.

These data were then used to determine the constants for the first three models discussed in the previous section which lend themselves to this type of analysis. With the Tuler-Butcher model, three calculations were performed. The value of λ was fixed at 1.0 and a least-squares fit was used to determine σ_0 and K. This was repeated with $\lambda = 2.0$. Finally σ_0 was set at 4.25 kilobars and values were found for λ and K. For the Rate Process model, a least-squares fit was used to find the two constants required. The Series Expansion model was limited to two time-dependent terms,

$$\sigma = \sigma_0 + \frac{A}{t} + \frac{B}{t^2} \tag{3}$$

and a least-squares fit was used to determine values for σ_0, A, and B. The pertinent equations used in the calculations are presented in appendix I. The results of these calculations are shown in table VII and figures 14 through 16.
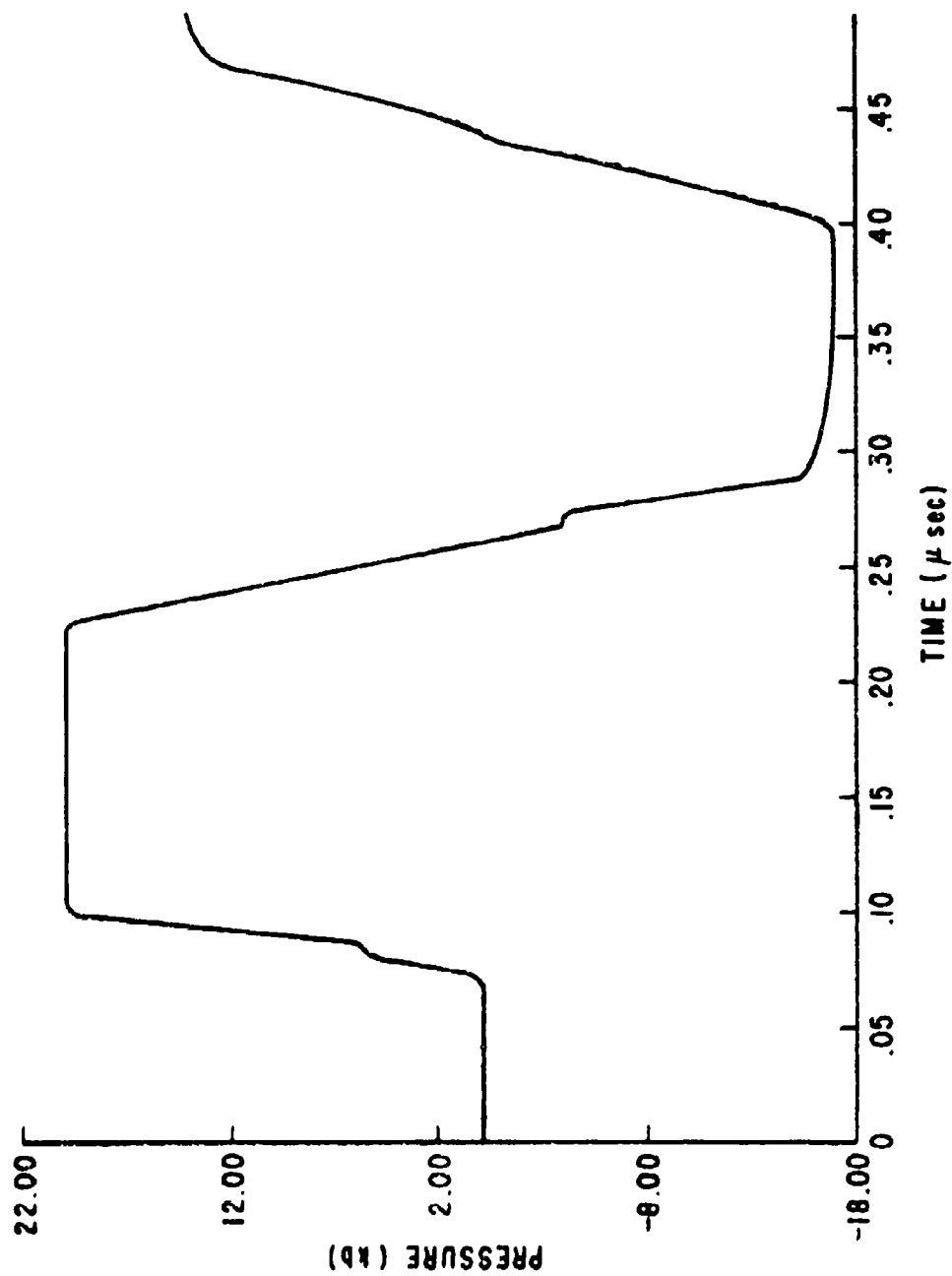
Figure 12. Stress-Time History at Spall Plane (AFWL)
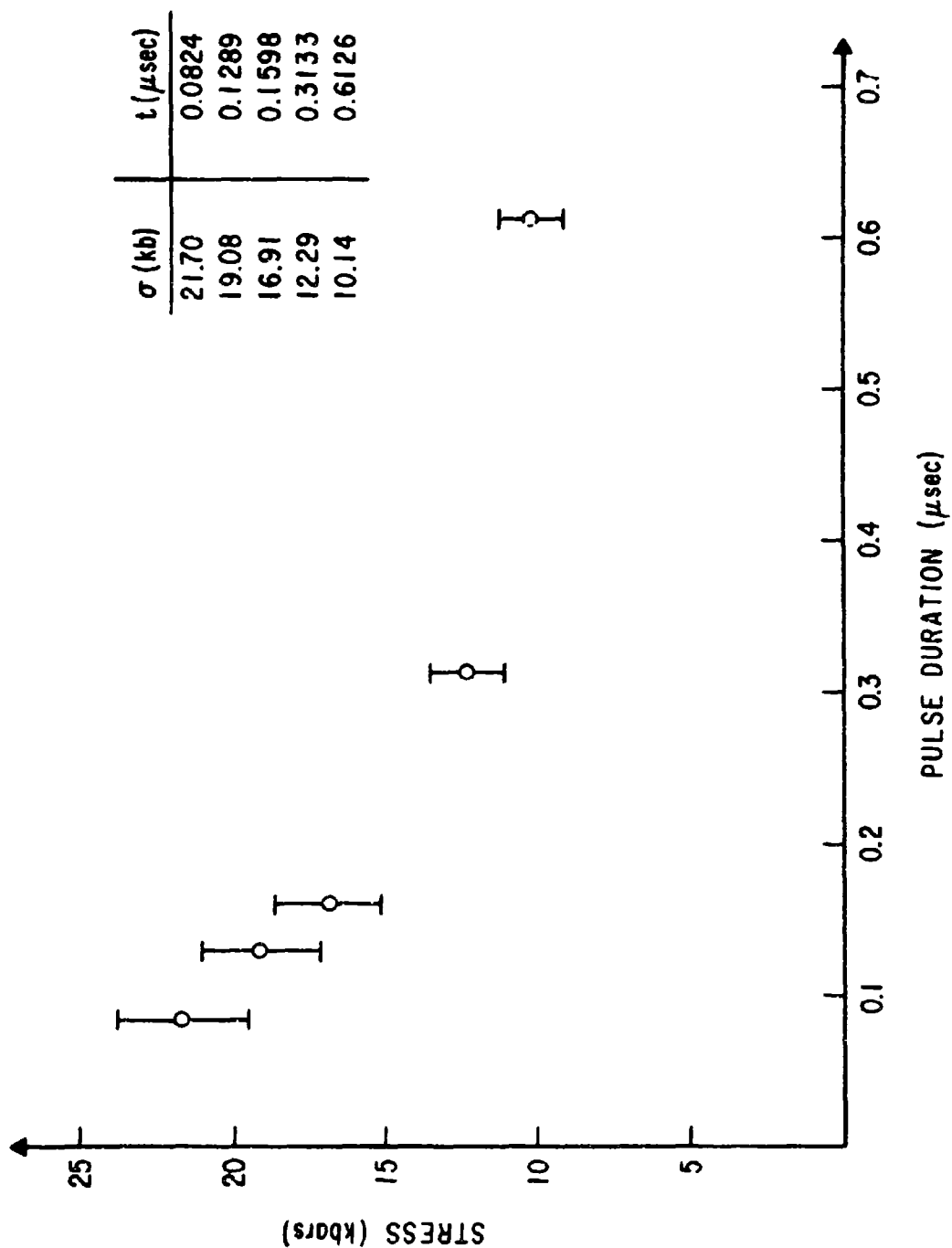
σ(kb)	t(μsec)
21.70	0.0824
19.08	0.1289
16.91	0.1598
12.29	0.3133
10.14	0.6126

STRESS (kbars)

PULSE DURATION (μsec)

Figure 13. Incipient Spall Threshold for 6061-T6 Aluminum

27

Table VII

CONSTANTS IN SPALL MODELS

Model*	Assumption	Variance**
Tuler-Butcher		
a. $(\sigma - 9.000)t = 1.134$	$\lambda = 1.0$	0.8098
b. $(\sigma - 2.995)^2 t = 5.504$	$\lambda = 2.0$	0.2227
c. $(\sigma - 4.25)^{1.81} t = 4.521$	$\sigma_o = 4.25$	0.2496
Rate Process		
a. $\sigma = 6.433 - 13.753 \log t$		0.4575
Series Expansion		
a. $\sigma = 6.630 + \dfrac{2.114}{t} - \dfrac{0.071}{t^2}$		0.0681

*Unit of stress is kilobars and unit of time is microseconds. Units of constants are consistent with these.
**The variance is a measure of the goodness-of-fit. It is the sum of the squares of the deviations averaged over the number of data points.

None of the models provides a bad fit of the experimental data. As Ferdman and Jajosky showed (Ref. 3) the Tuler-Butcher model provides a better fit with $\lambda = 2$ than with $\lambda = 1$. Also, for fixed σ_0, the best fit value for λ is closer to two than to one. The Tuler-Butcher model provides a somewhat better fit than the Rate Process model. The Series Expansion model obviously provides the best fit, although the negative value of the constant B leads to an unrealistic behavior of the spall threshold at very short pulse duration.

The next step in the evaluation of these models was to include more of the spall data available for 6061-T6 aluminum. The data used are summarized in table VIII.

Some discussion of these data is appropriate before applying any of the models. The data from GM have been mentioned previously. It was obtained under the PREDIX program using the same experimental technique as the AFWL used. The Sandia
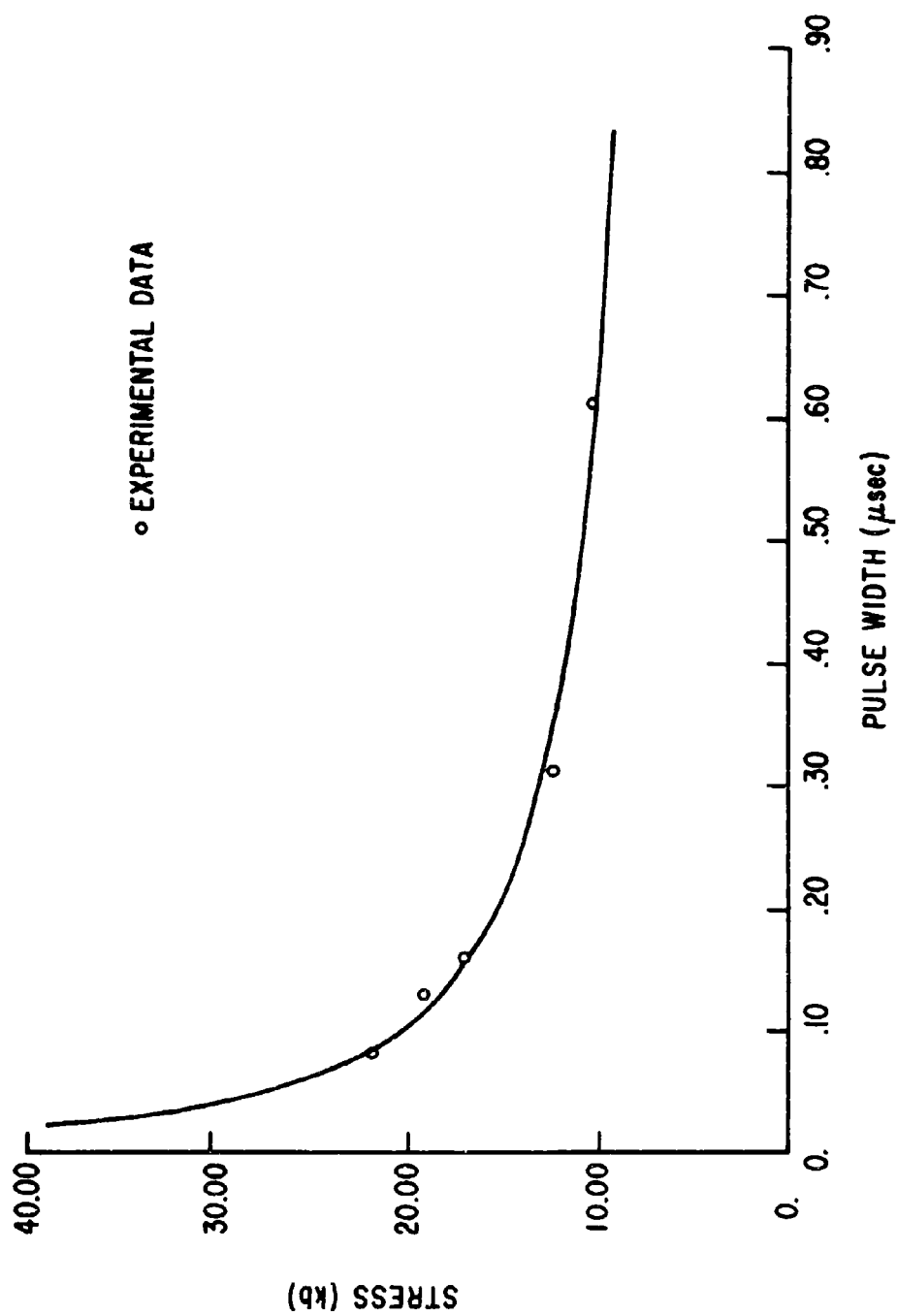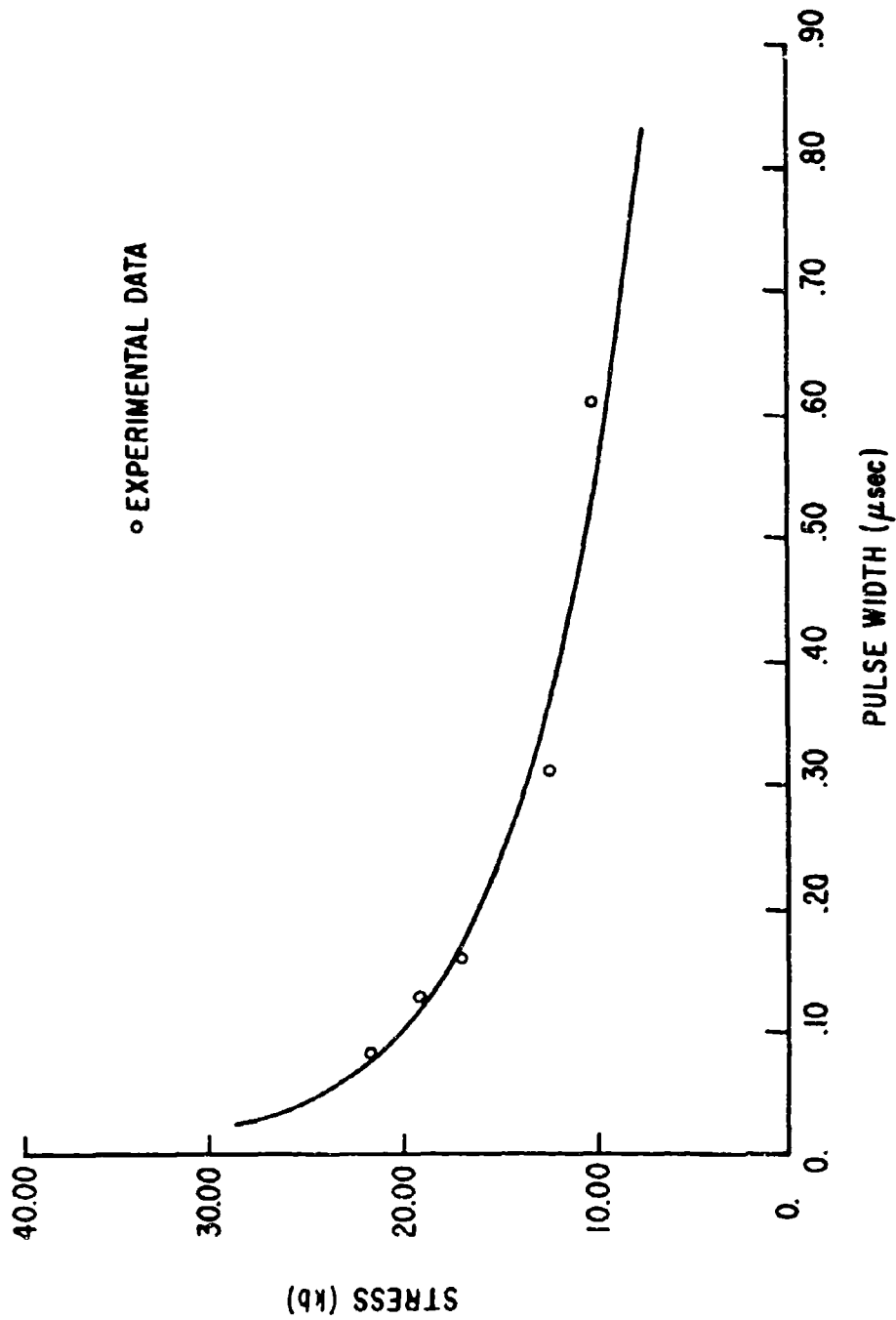
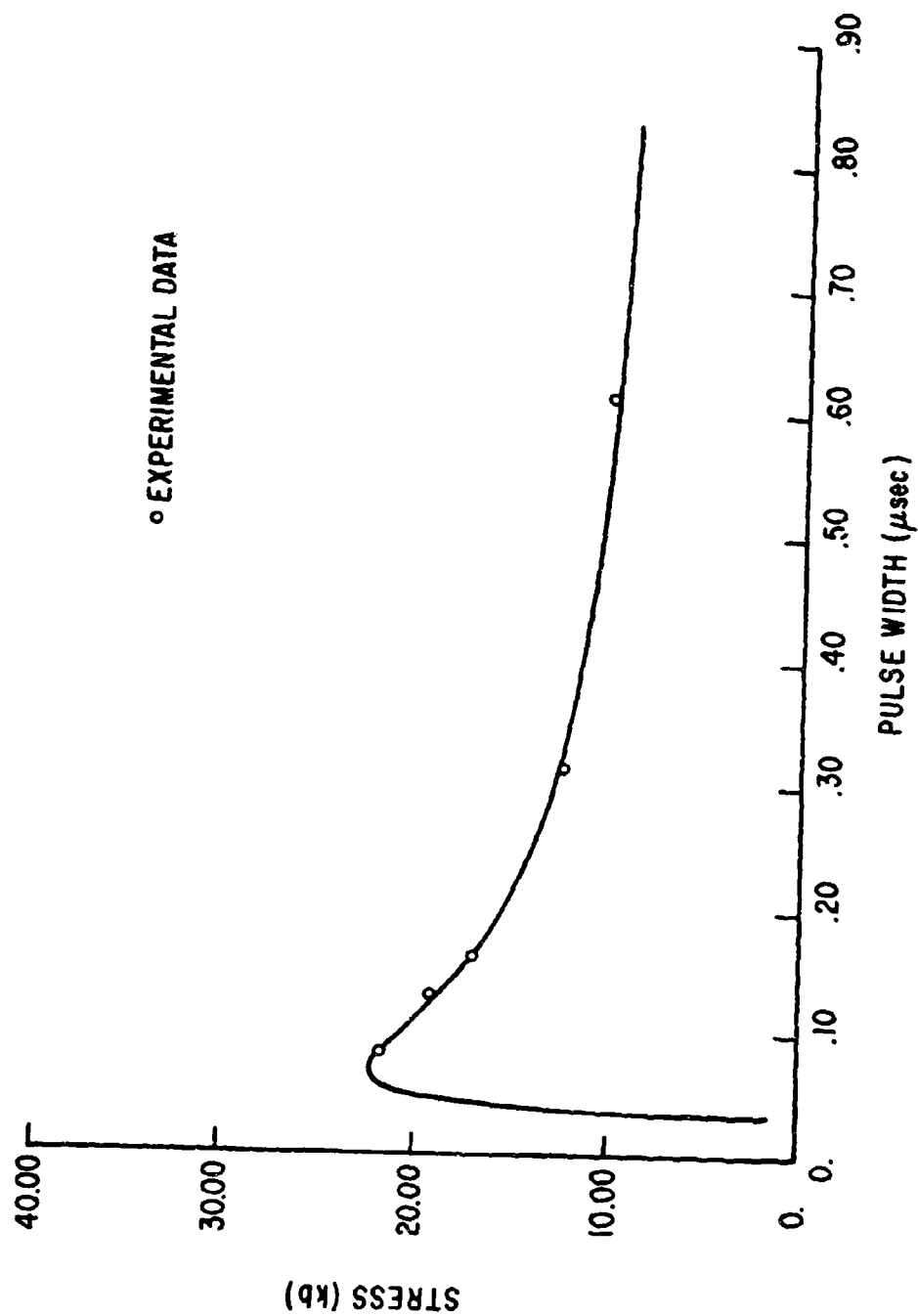Figure 14. Tuler-Butcher, $\lambda = 2.0$

Figure 15. Rate Process Model

30

Figure 16. Series Expansion Model

Table VIII

6061-T6 ALUMINUM SPALL DATA
(AT ROOM TEMPERATURE)

Lab (Ref.)	Flyer Thick (cm)	Target Thick (cm)	Velocity (cm/sec)	Peak Stress (kb)	Pulse Duration (μ sec)	Pulse Shape
AFWL	0.0254	0.0508	33200	21.70	0.0824	Rectangular
	0.0406	0.0813	29200	19.08	0.1289	Rectangular
	0.0508	0.1016	26000	16.91	0.1598	Rectangular
	0.1016	0.2032	18900	12.29	0.3133	Rectangular
	0.2032	0.4064	15600	10.14	0.6126	Rectangular
GM (1)	0.025	0.050	26200	17.26	0.0774	Rectangular
	0.050	01.00	22000	14.35	0.1461	Rectangular
	0.150	0.300	19000	12.84	0.4056	Rectangular
	0.273	0.546	17500	11.43	0.7470	Rectangular
	0.400	0.800	16500	10.54	1.0890	Rectangular
Sandia (20)	0.159	0.635	19800	12.58	0.5395	Rectangular
	0.315	1.270	16500	10.60	0.8216	Rectangular
	0.635	2.540	13000	8.82	1.7241	Rectangular
ETI (19)	0.013*	0.328	112000	19.30	0.0894	Triangular
	0.024*	0.638	83000	9.20	0.1892	Triangular
Boeing (21)	0.076	0.305	28000	17.93	0.2956	Rectangular
	0.254	1.020	19000	12.11	0.6957	Rectangular
	0.508	2.030	13500	8.92	1.3514	Rectangular
MDAC (13)	0.0127*	0.0813	98000	30.80	0.0566	Triangular
	0.0190*	0.0813	83000	26.19	0.1254	Rectangular
	0.0254*	0.0813	72000	21.75	0.1370	Rectangular
ETI (22)	0.0127*	0.0508	65000	18.52	0.0826	Rectangular
	0.0127*	0.3175	115000	16.48	0.1865	Triangular
Sandia (13)	0.2540	1.0120	16000	10.37	0.6849	Rectangular
	0.0826	0.3300	21000	13.36	0.2926	Rectangular
AFRTD (23)	0.0235	0.0940	30800	19.87	0.0947	Rectangular
	0.0823	0.3300	28500	18.28	0.3263	Rectangular
	0.1585	0.6350	25300	16.13	0.6085	Rectangular
	0.2350	0.9400	21500	13.56	0.8382	Rectangular
	0.3175	1.2700	18700	11.89	0.8941	Rectangular
	0.4775	1.9100	12200	8.30	1.2778	Rectangular
	0.6350	2.5400	10000	7.28	1.6047	Rectangular
AFWL (3)	0.0191*	0.0813	84000	30.40	0.1170	Rectangular
	0.0254*	0.0813	65000	23.20	0.1330	Rectangular

*Mylar flyers.

32

points were also obtained with a gas gun, but the target-to-flyer thickness ratio was 4:1 as it was in the Boeing experiments. The ETI points were obtained with an exploding-foil apparatus under the PREDIX program. The thickness ration was 25:1 and the pulses were essentially triangular. McDonnell Douglas Astronautics Company used an exploding foil apparatus and a variable thickness ratio. The last two points were obtained by Ferdman and Jajosky also with an exploding foil. Although some of these results are relatively old and different definitions of incipient spall were used, all data points were assigned equal weights. No attempt was made to provide more recent data with greater significance in the analyses. The P-PUFF computer code was used to reduce the data to peak tensile stress and pulse duration. Representative stress-time histories for each data set are shown in figure 17 through 25. Figure 26 is a plot of the spall threshold showing the large experimental scatter especially for very short pulse durations. Each of the models was again fit to the data with the results shown in table IX and figures 27 through 28.

The results of this analysis are not surprising. Because of the scatter in the available data, all the models fit the data reasonably well. This is obvious from the variances listed in table IX and from an examination of figure 27. More discussion of this point is presented in the final section.

3. FRACTURE CALCULATIONS

As previously mentioned in this report, the goal of the impact experiments was to obtain spall data on 6061-T6 aluminum which could be used to evaluate various mathematical models of dynamic fracture for inclusion in PUFF-type computer codes to enhance their predictive capabilities. At the time of these experiments, the PUFF fracture criterion was critical tensile stress, which has been shown to be an unrealistic criterion for materials of interest.

To determine the adequacy of the models considered for predicting dynamic fracture, it is necessary to incorporate them into a PUFF-type code and compare

Figure 17. Stress-Time History at Spall Plane (GM)

Figure 18. Stress-Time History at Spall Plane (Sandia)

35

Figure 19. Stress-Time History at Spall Plane (ETI)

Figure 20. Stress-Time History at Spall Plane (Boeing)

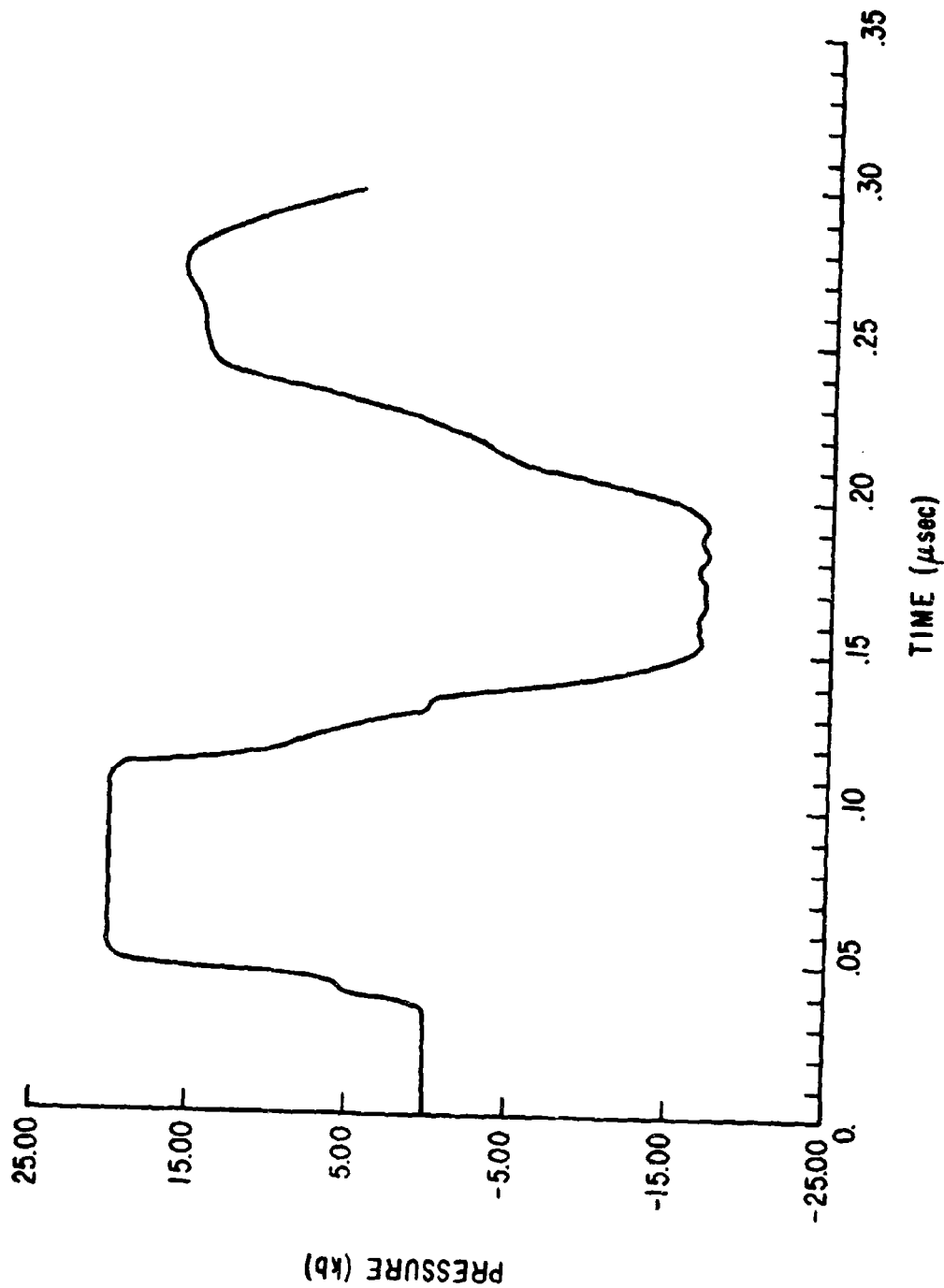Figure 21. Stress-Time History at Spall Plane (MDAC)

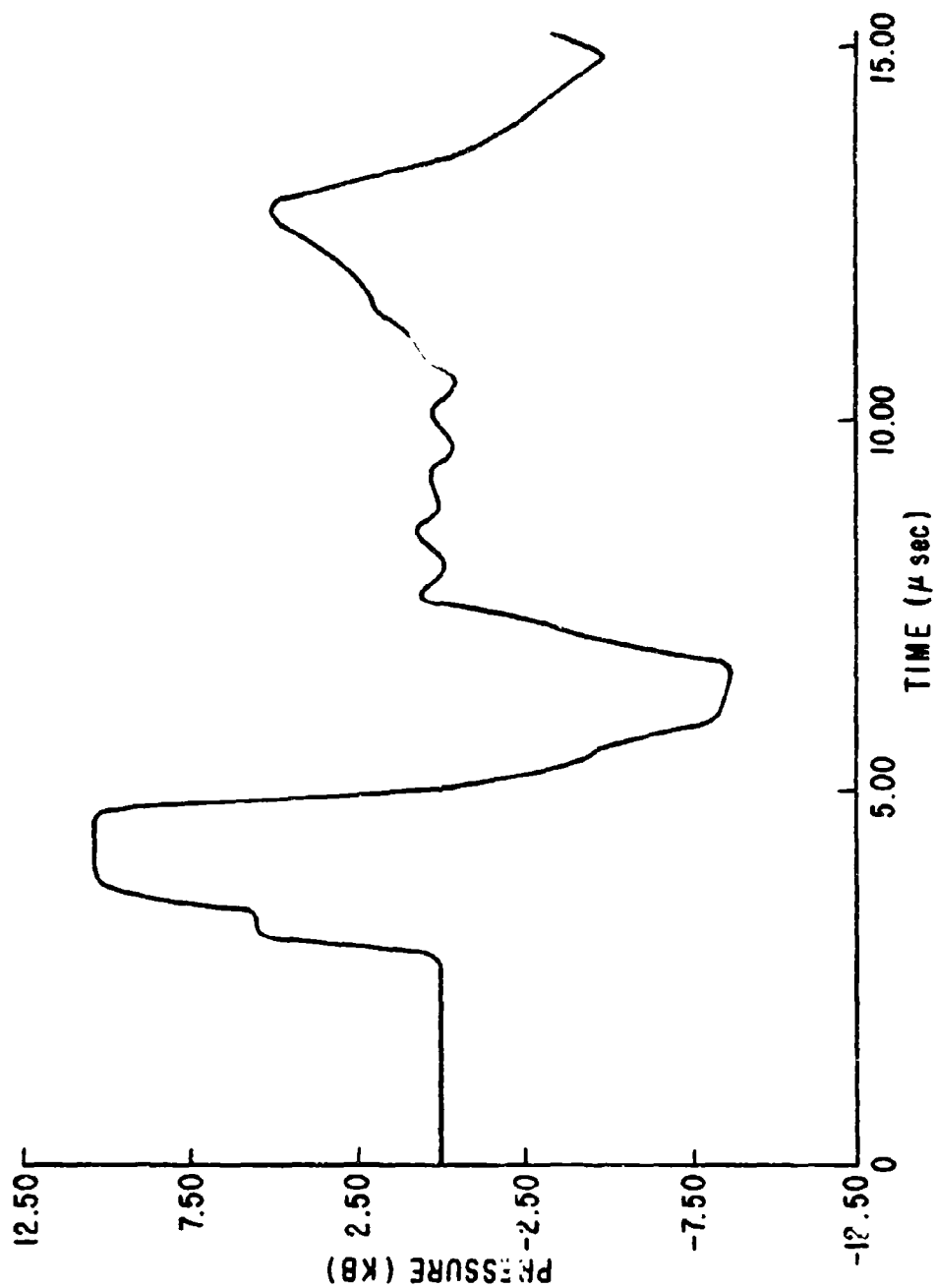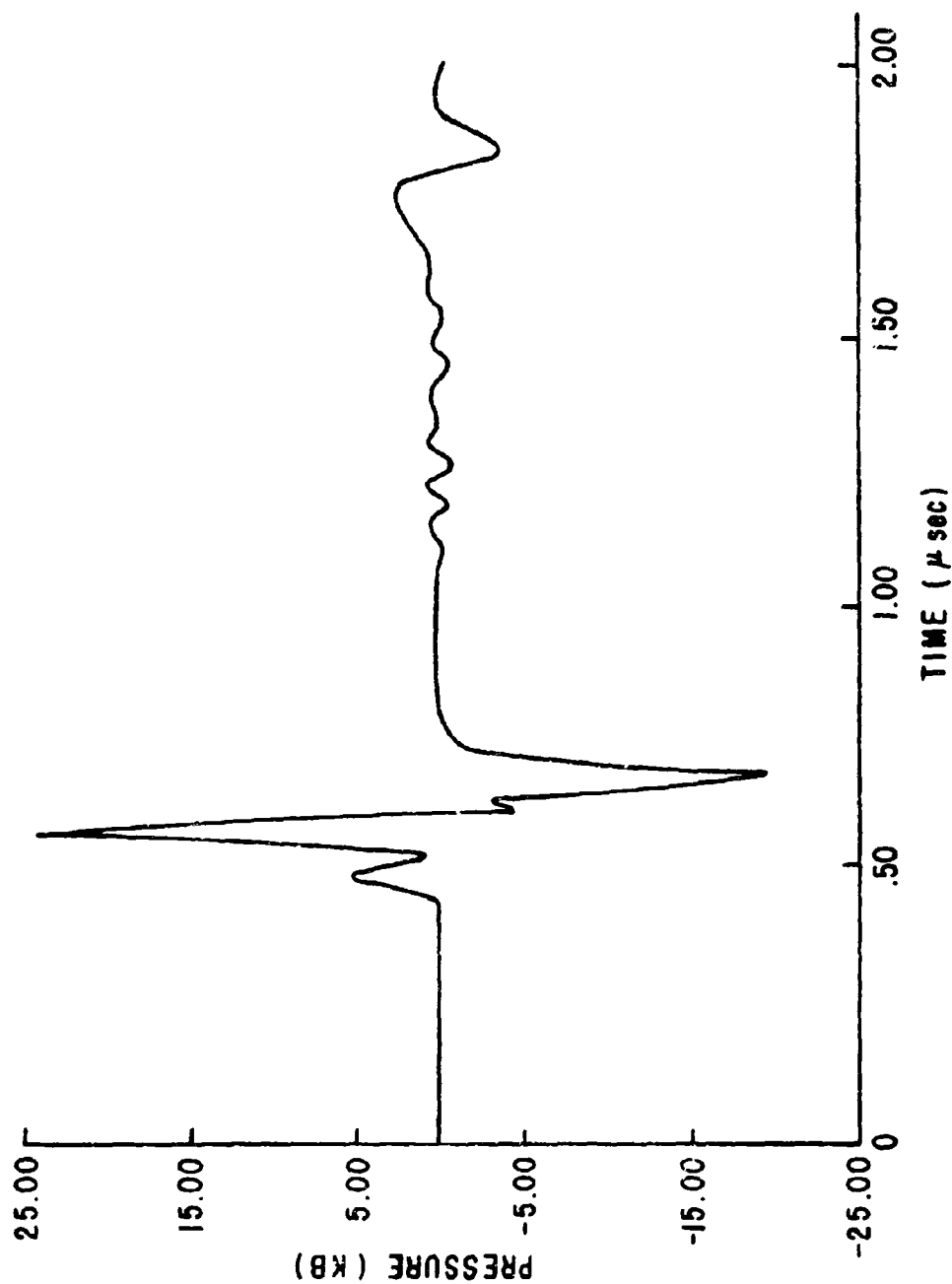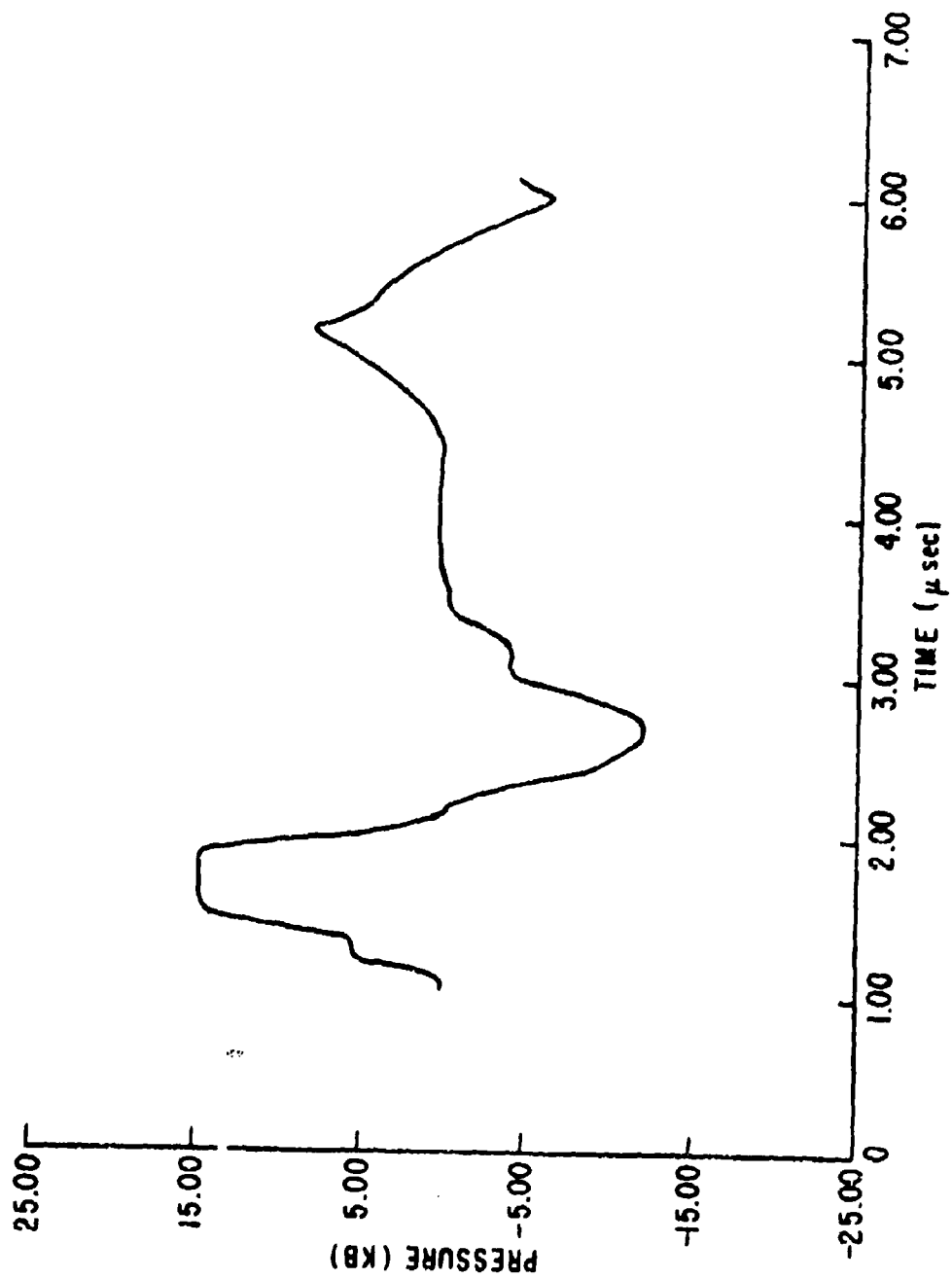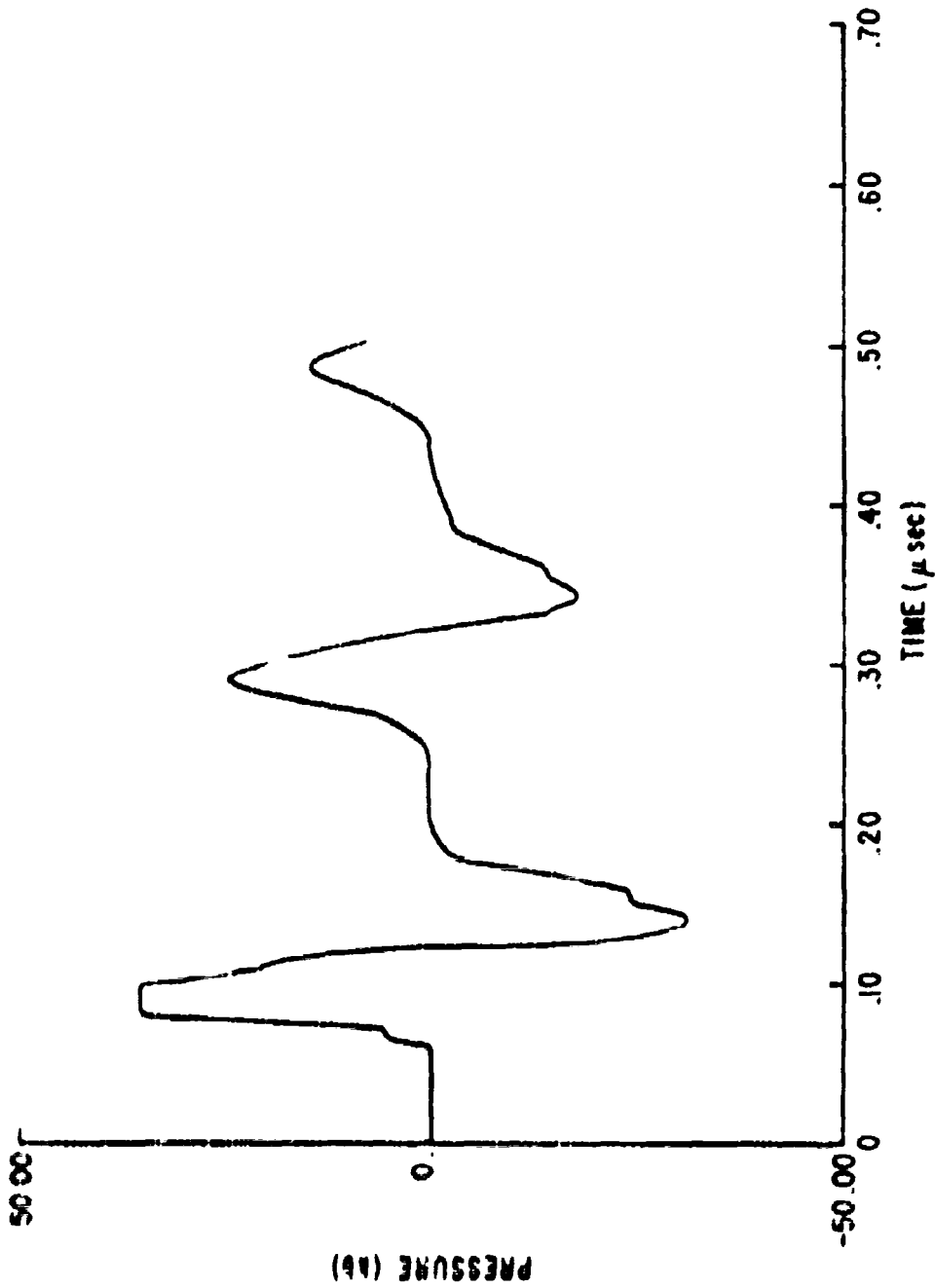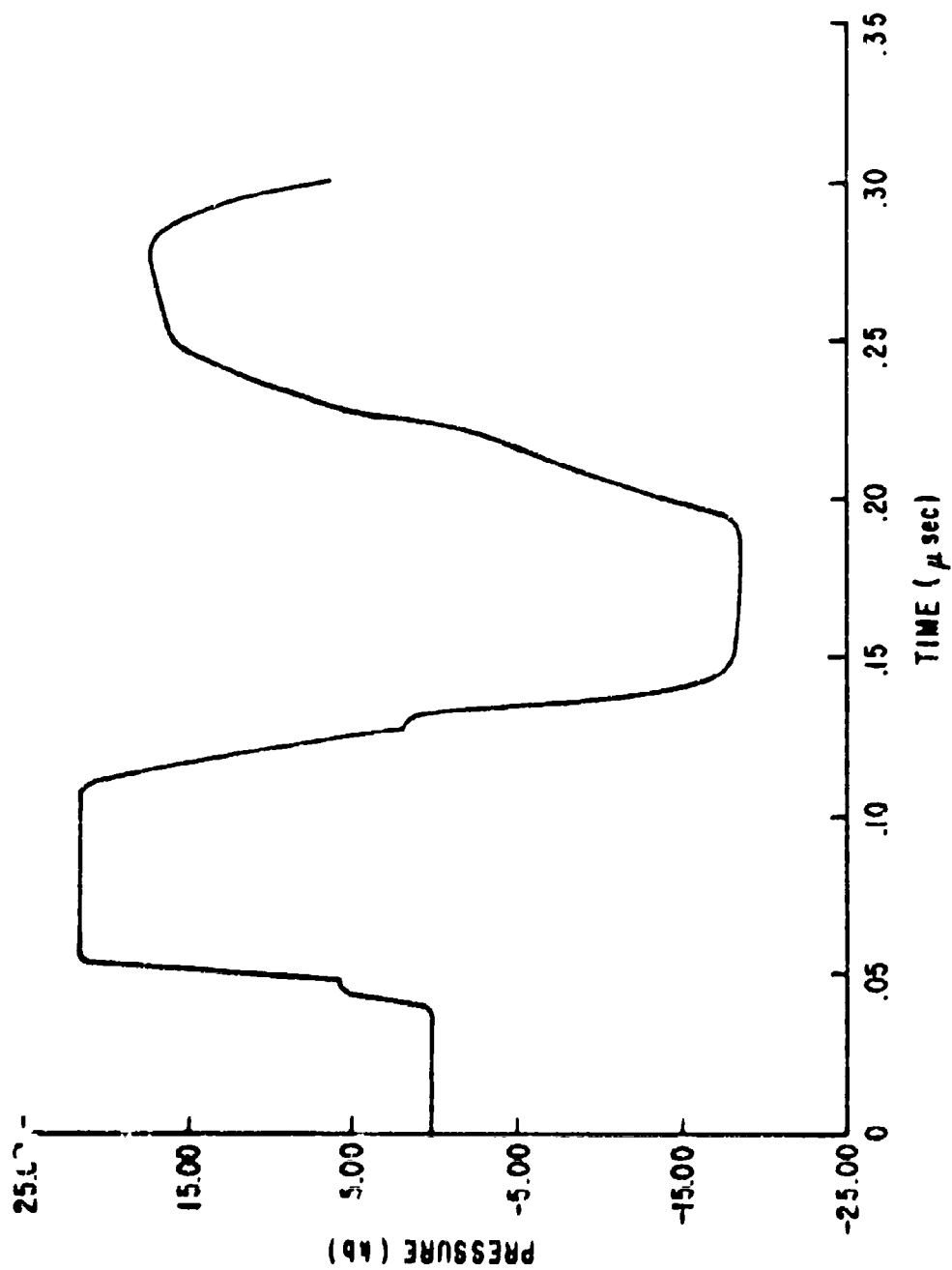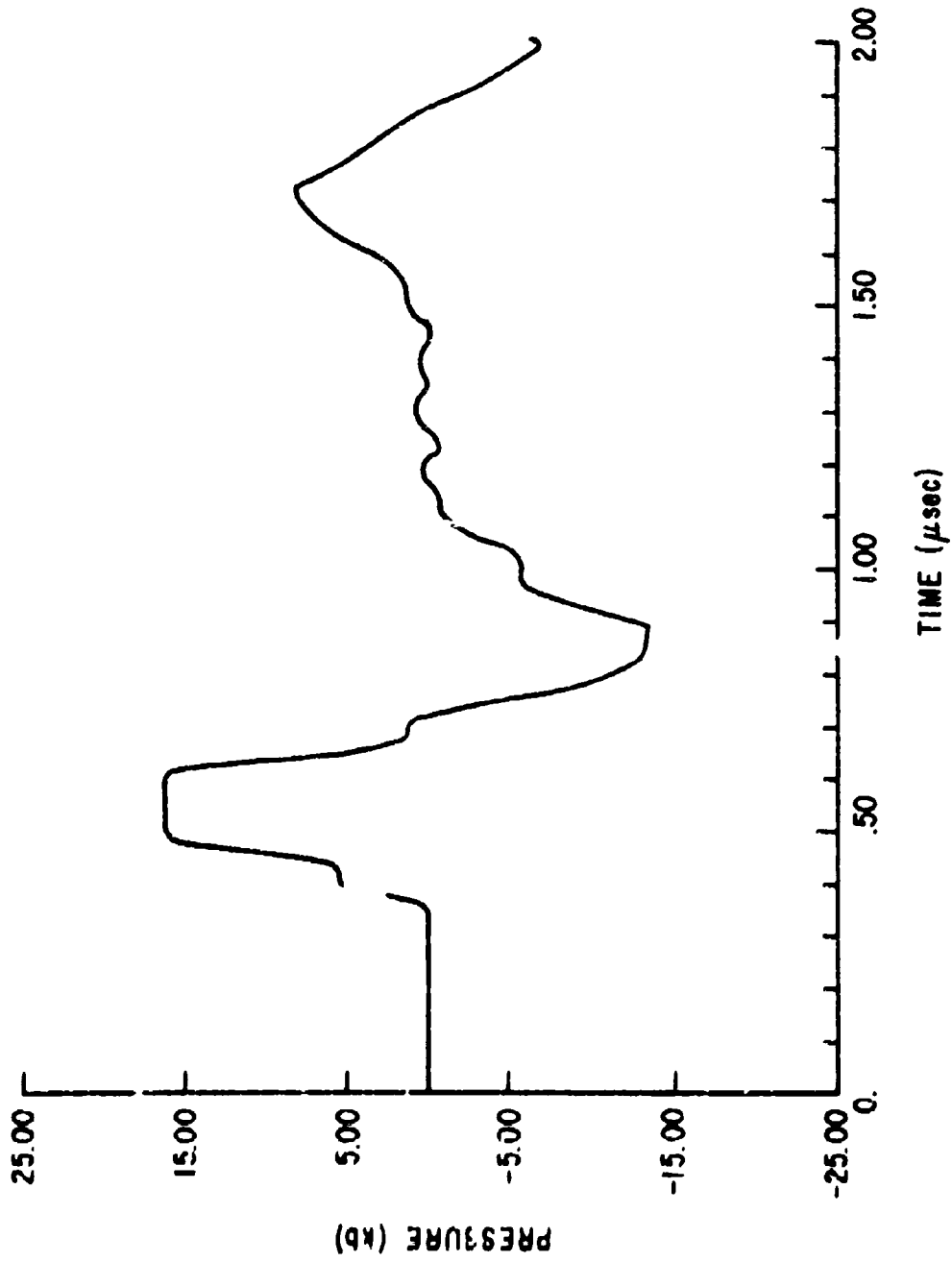Figure 22. Stress-Time History at Spall Plane (ETI)

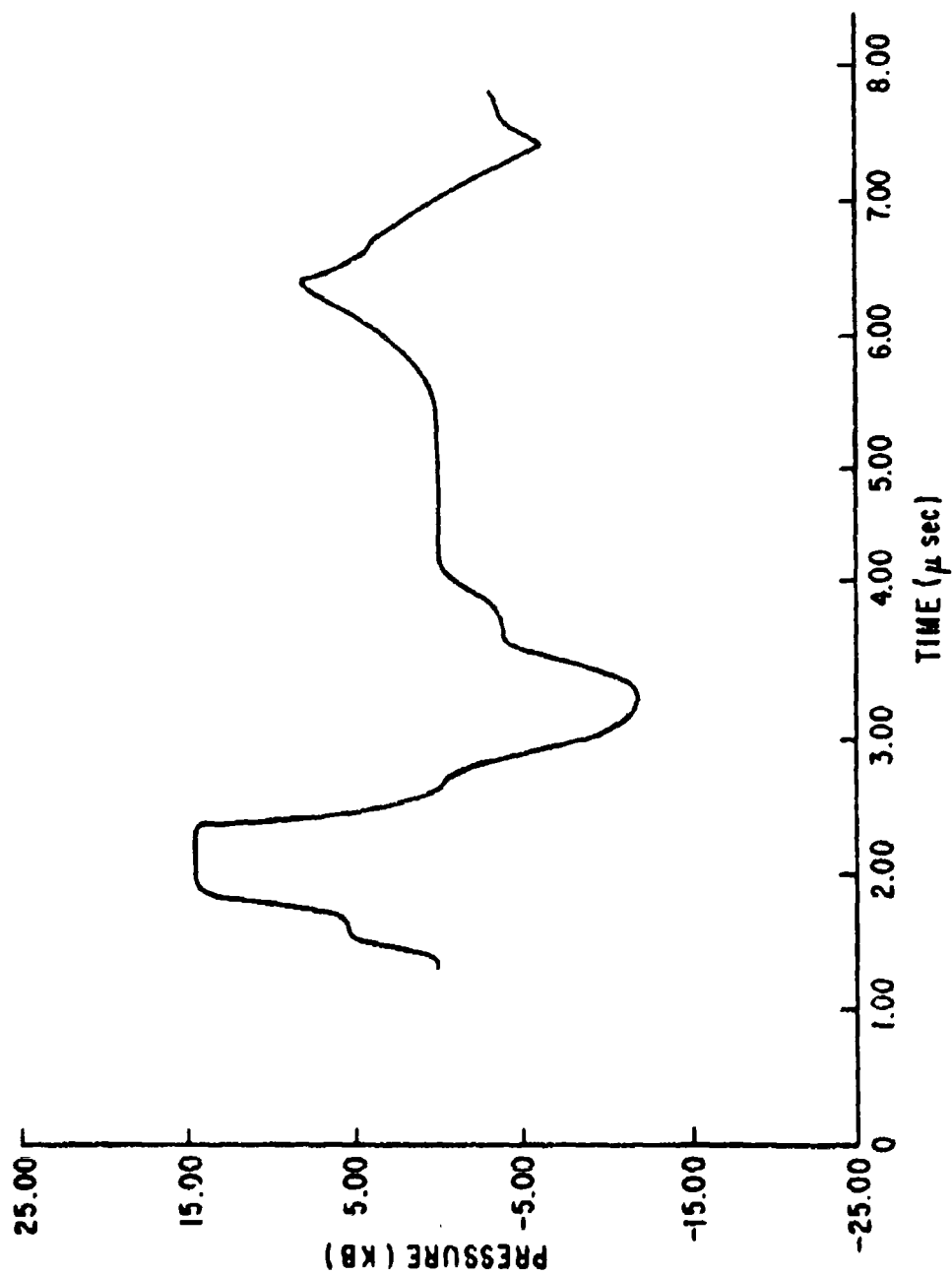Figure 23. Stress-Time History at Spall Plane (Sandia)
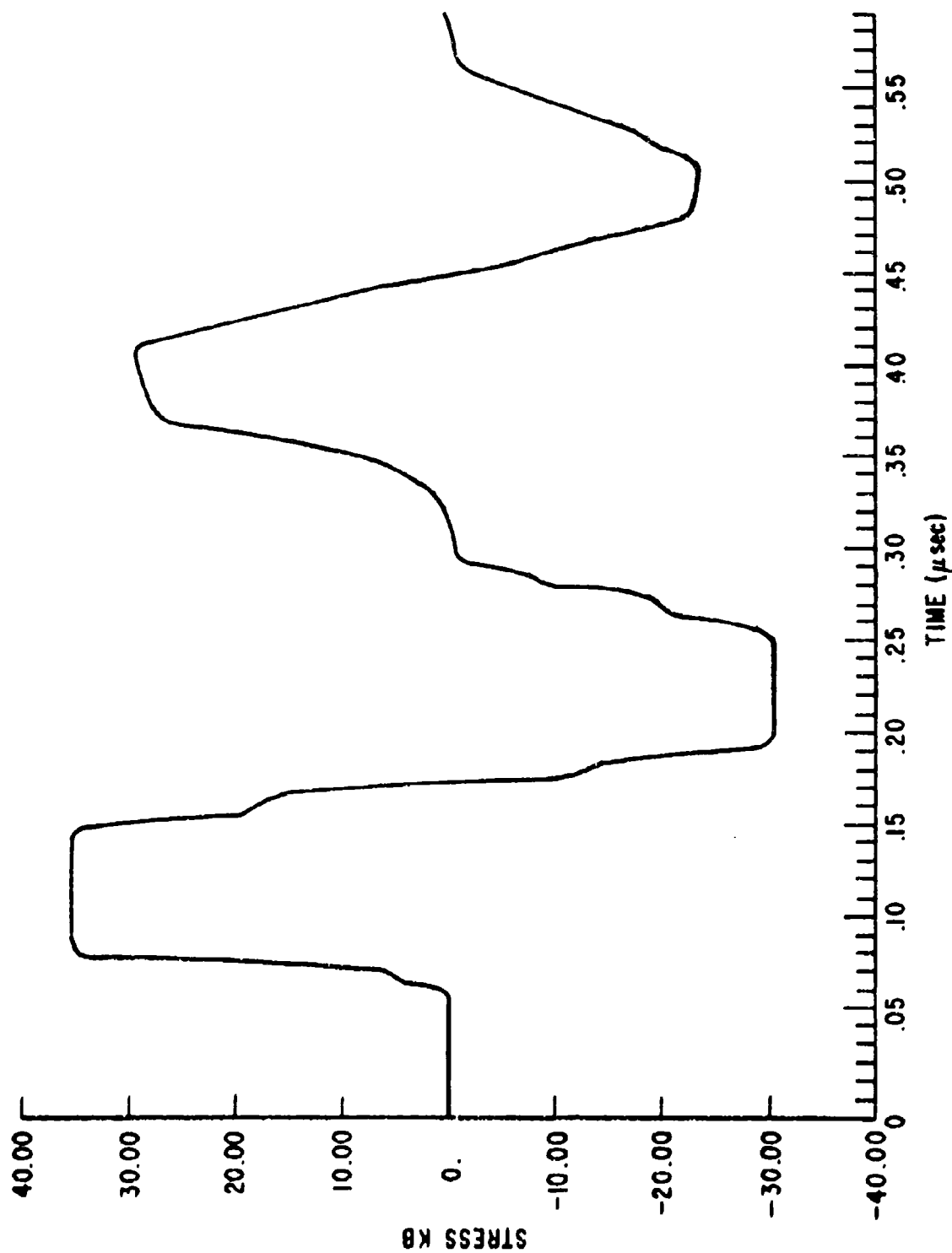
Figure 24. Stress-Time History at Spall Plane (AFRTD)
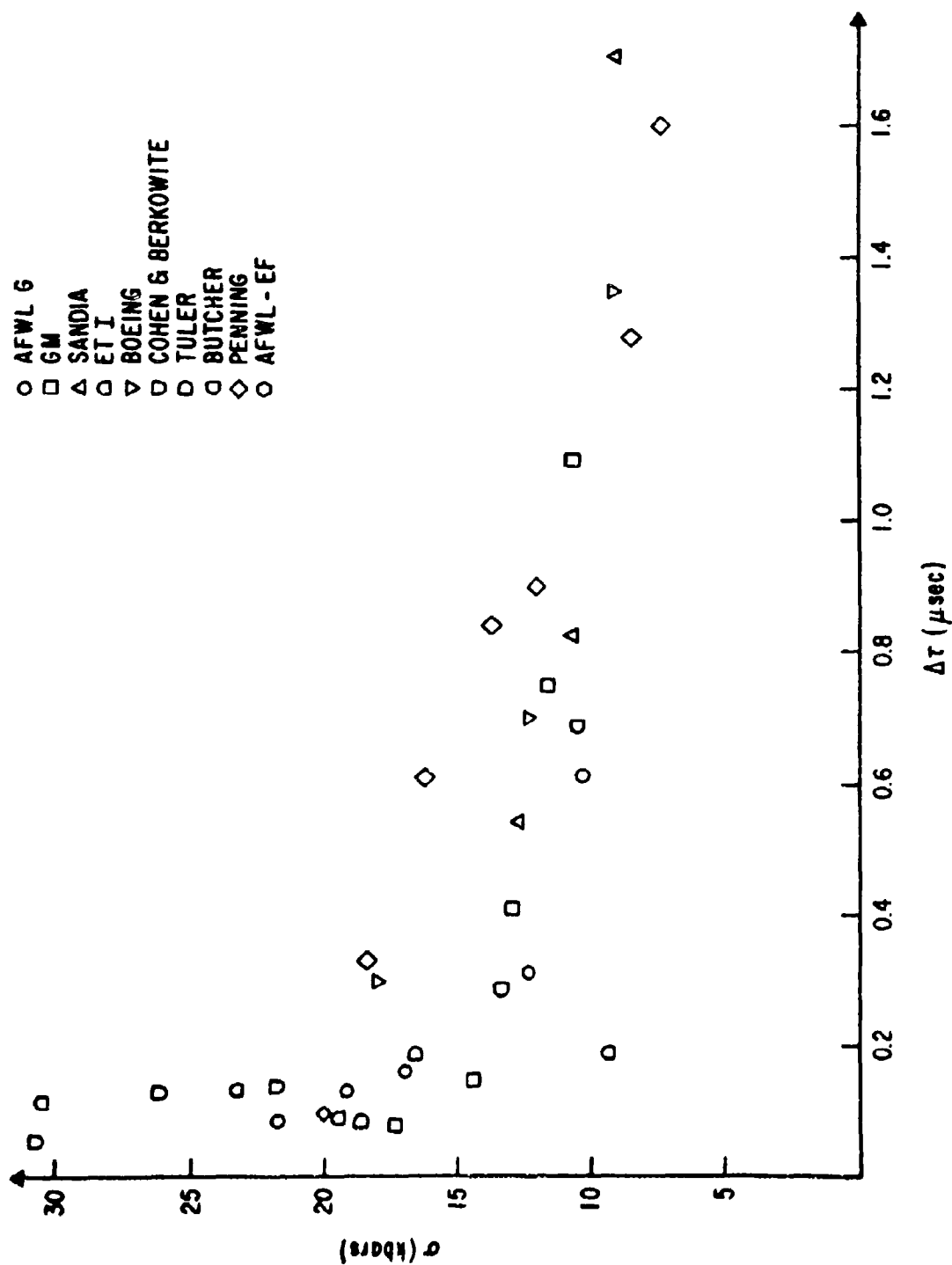
Figure 25. Stress-Time History at Spall Plane (AFWL)

Figure 26. 6061-T6 Aluminum Spall Data

43

Table IX

SPALL MODEL CONSTANTS

Model	Assumption	Variance
Tuler-Butcher		
a. $(\sigma - 10.206)t = 1.069$	$\lambda = 1.0$	13.0844
b. $(\sigma - 5.487)t = 4.979$	$\lambda = 2.0$	12.1187
c. $(\sigma - 4.250)^{2.27}t = 6.154$	$\sigma_0 = 4.25$	12.0973
Rate Process		
a. $\sigma = 10.011 - 10.906 \log t$		12.6634
Series Expansion		
a. $\sigma = 9.255 + \dfrac{1.557}{t} - \dfrac{0.034}{t^2}$		12.5860

experimental results with results calculated using each of the models. Thus, the first three models described in table V were substituted for critical tensile stress in the AFWL P-PUFF code. The changes required in the code are presented in appendix II. A version of SRI PUFF 3 with the Hole-Growth model as a fracture criterion was available and was used for the evaluation of this model.

Sample runs were made for each model using 0.020 inch of aluminum impacting 0.040 inch of aluminum. Two impact velocities were used for each model such that results should have included both no-damage and incipient spall. According to AFWL experimental results, an impact velocity of 0.20 mm/μsec should not have resulted in any damage while a velocity of 0.26 mm/μsec was required for incipient spall.

Before discussing the results of the computations, it should be noted that some difficulties were encountered in attempting to compare calculations based on the first three models with those based on the Hole-Growth model. These difficulties arose from inherently different descriptions of fracture.
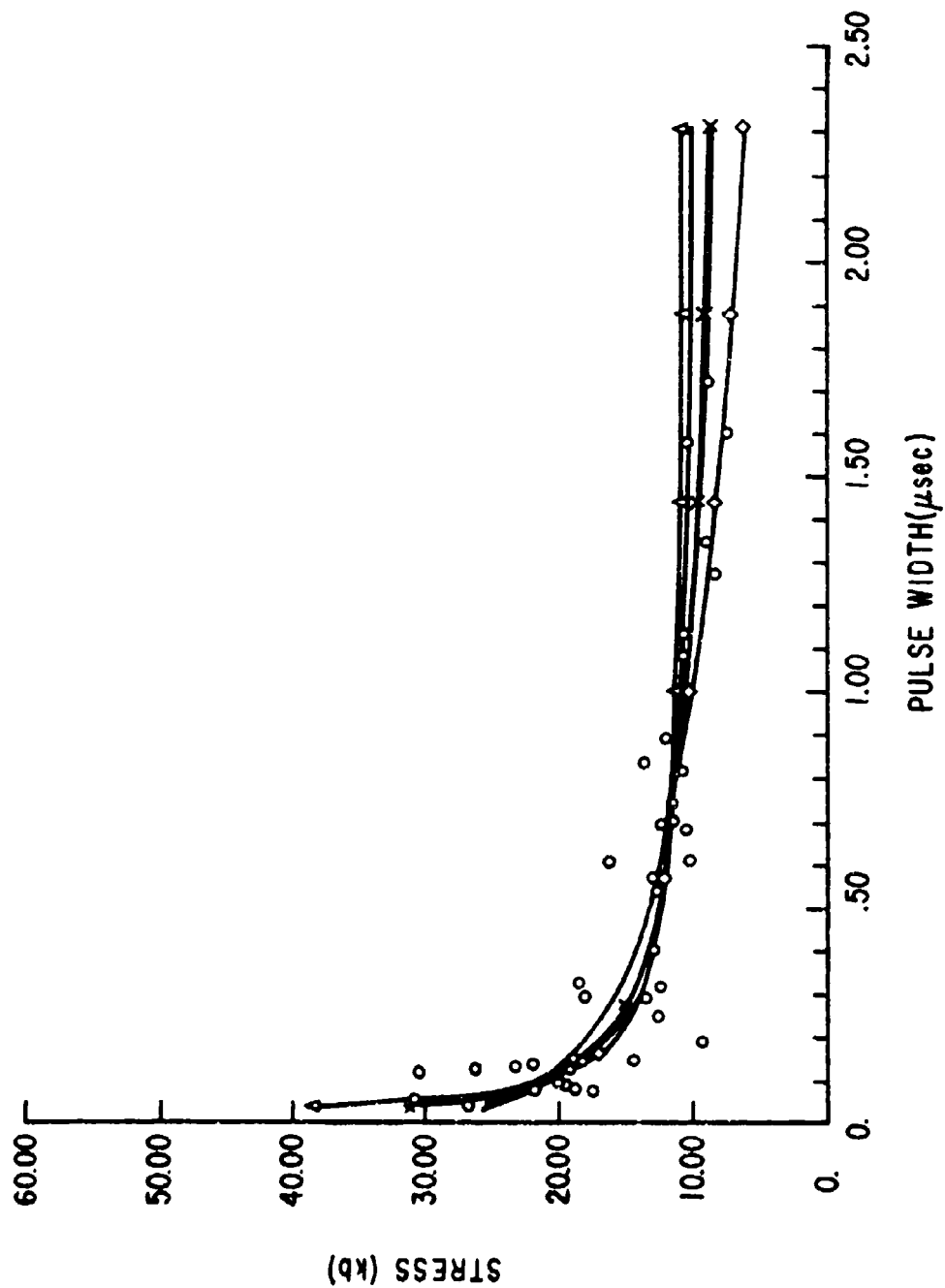
Figure 27. Comparison of Spall Models and Experimental Data
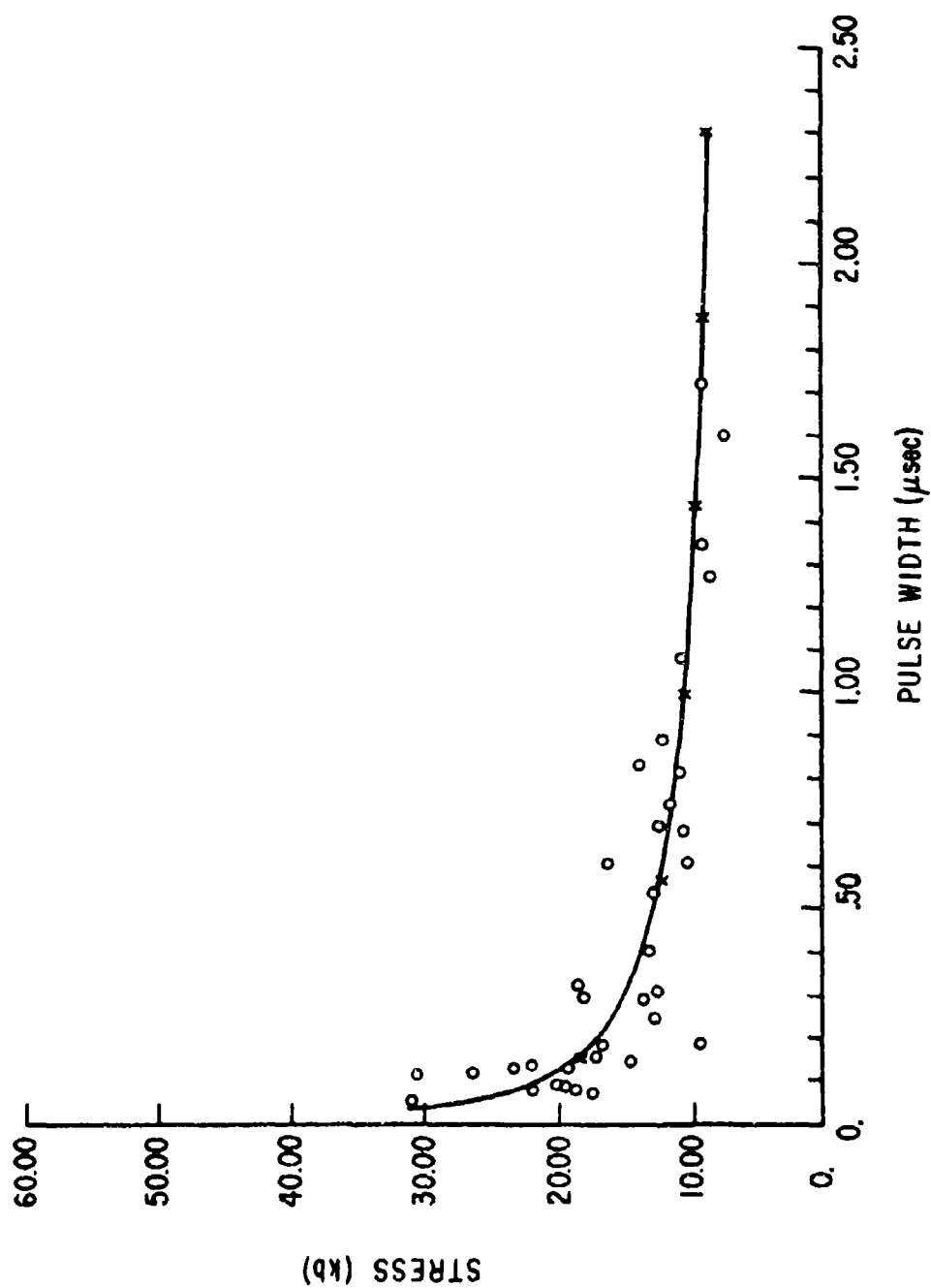
Figure 28. Comparison of Tuler-Butcher Model and Experimental Data

PUFF and P-PUFF are one-dimensional Lagrangian hydrodynamic codes which calculate propagation of stress waves through a layered homogeneous material using finite difference methods. The existing fracture routine handles spall by creating and deleting free surfaces at zone boundaries when certain criteria are met. There are no real provisions for levels of damage which represent less than complete separation of the material. Obviously, this is not physically realistic since damage may range from a single microcrack to complete separation.

The Hole-Growth model, however, is capable of describing various levels of damage within a given zone by either increasing void density or increasing void volume. Thus, in discussing the results of fracture computations, it is appropriate to postpone those for the SRI Hole-Growth model until later in the section. The other three models are similar in format and lend themselves to simultaneous discussion.

Table X presents the results of sample runs using two versions of the Tuler-Butcher model as well as the Rate Process and Series Expansion models. All four models used resulted in some spall even at the low velocity. The Tuler-Butcher model appeared to be relatively insensitive to impact velocity allowing the lowest velocity impact to spall as severely as the incipient shot. The Rate Process and Series Expansion models were better, but not good.

The problem which arose in the interpretation of these results was the definition of level of damage in the computer calculations. It was not clear whether one spalled zone should be defined as below incipient spall, incipient spall, or complete spall. However, no immediate decision was made on this question because of the discouraging results of the computed shots.

To test the sensitivity of the calculations to errors in the experimentally determined constants, additional computer runs were made with the constants of each model individually varied by 5 percent in such a way as to decrease the number of spalled zones which resulted. The Tuler-Butcher model, as expected,

Table X

NUMBER OF SPALLED ZONES COMPUTED BY FRACTURE MODELS*

Model	.20 mm/μsec	.26 mm/μsec	.31 mm/μsec
Tuler Butcher, $\lambda = 1.81$	19	20	--
Tuler Butcher, $\lambda = 2.00$	22	22	--
Rate Process	20	26	--
Series Expansion	13	17	27

*Targets all contained 200 zones.

was most sensitive to the value selected for λ. A 5 percent change in any other constant did not appreciably affect the computed results for any of the models. Thus, the conclusion was that none of these models could provide much more than a crude approximation of dynamic failure in homogeneous materials of interest.

The Hole-Growth model, however, provided more encouraging results. Experimentally determined values for the fracture parameters were not available for the 6061-T6 aluminum at the time of this work. The values used were approximations based on values determined for 1145 aluminum by SRI (Ref. 4). The SRI analysis is based on nucleation and growth of voids where the nucleation rate is

$$\dot{N} \ (\sigma, \ t) = B \ (\sigma - \sigma_N) \tag{4}$$

and the growth rate is

$$\dot{R} \ (\sigma, \ t) = C \ (\sigma - \sigma_G) \ R \tag{5}$$

A comparison of the behavior of 6061-T6 aluminum undergoing dynamic failure with that of 1145 aluminum reveals a number of characteristics useful in approximating the unknown fracture parameters. Both materials undergo ductile dynamic failure indicating that the same failure models are applicable. Studies of 1145 aluminum indicated that voids were nucleated at inclusion sites, but that the number of potential sites was far greater than the number of voids observed. Thus, even though the 6061-T6 aluminum provides a still greater number of potential

nucleation sites, no appreciable change in the value of B in equation (4) should be required.

However, the threshold stress for nucleation, σ_N, should be somewhat higher than that for 1145 aluminum. 6061-T6 aluminum does require slightly higher stresses to cause a given level of damage. This is due to its greater yield strength which will affect the threshold stress for both nucleation and growth.

Finally, growth is related to both yield strength and the viscosity of a material. The growth coefficient is inversely proportional to the viscosity η. Mitchell, Hauser and Dorn (Ref. 24) have shown that η is higher for 6061-T6 aluminum. Thus the growth coefficient C should be somewhat lower.

The values used in the computer calculations are summarized in table XI. The results of these computations are illustrated in figure 29. This figure also shows photomicrographs of 0.040-inch targets impacted at the velocities used in the calculations.

Table XI

FRACTURE PARAMETERS FOR 6061-T6 ALUMINUM

B	-	5.0×10^{5} No./dyne-cm-sec
σ_N	-	8.0×10^{9} dynes/cm^2
C	-	1.5×10^{-3} cm^2/dyne-sec
σ_G	-	4.0×10^{9} dynes/cm^2

From figure 29, it is apparent that the threshold for incipient spall should be defined as a void volume of approximately 2.5 percent of original material volume. To further verify this observation, additional calculations were performed for each of the AFWL data points. Results are shown in figure 30 with photomicrographs of actual damage. Since all damage levels are approximately incipient spall, the threshold for this level of damage might be defined as void volumes of 2.2 to 3.5 percent for this material.

49
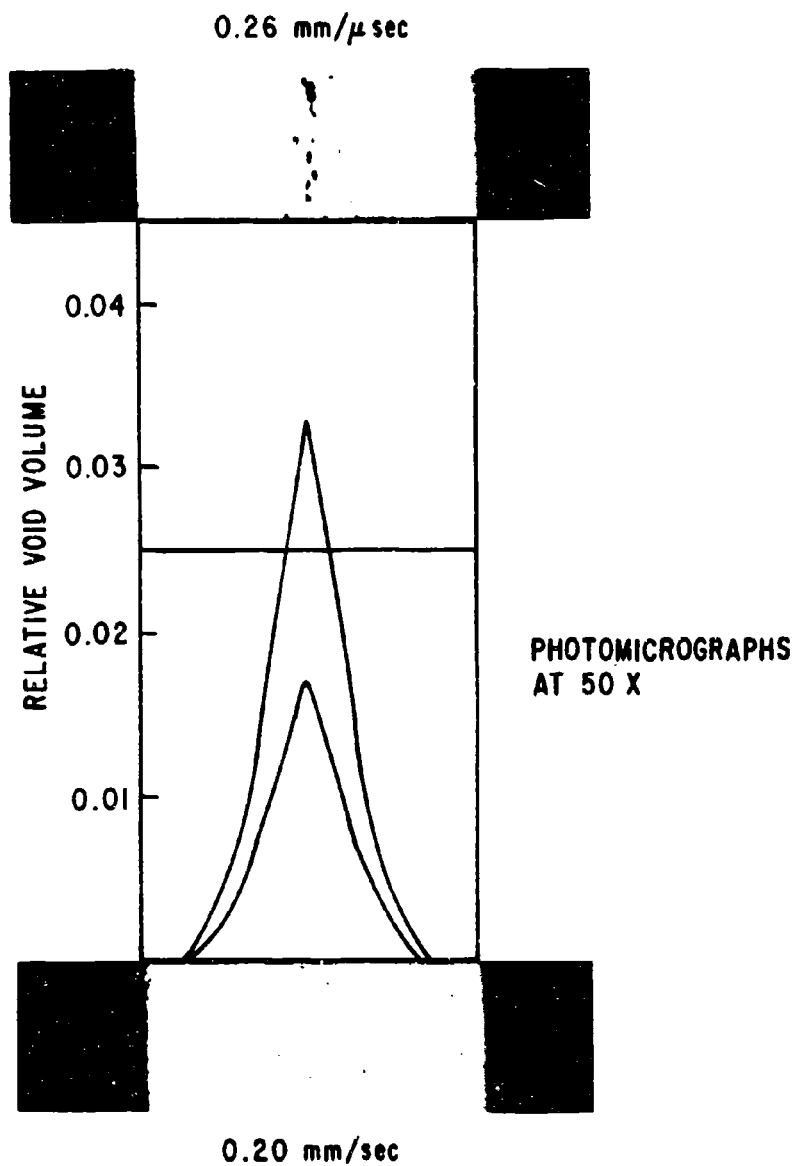
Figure 29. Damage Levels Calculated with
Hole-Growth Model for 40 Mil Target
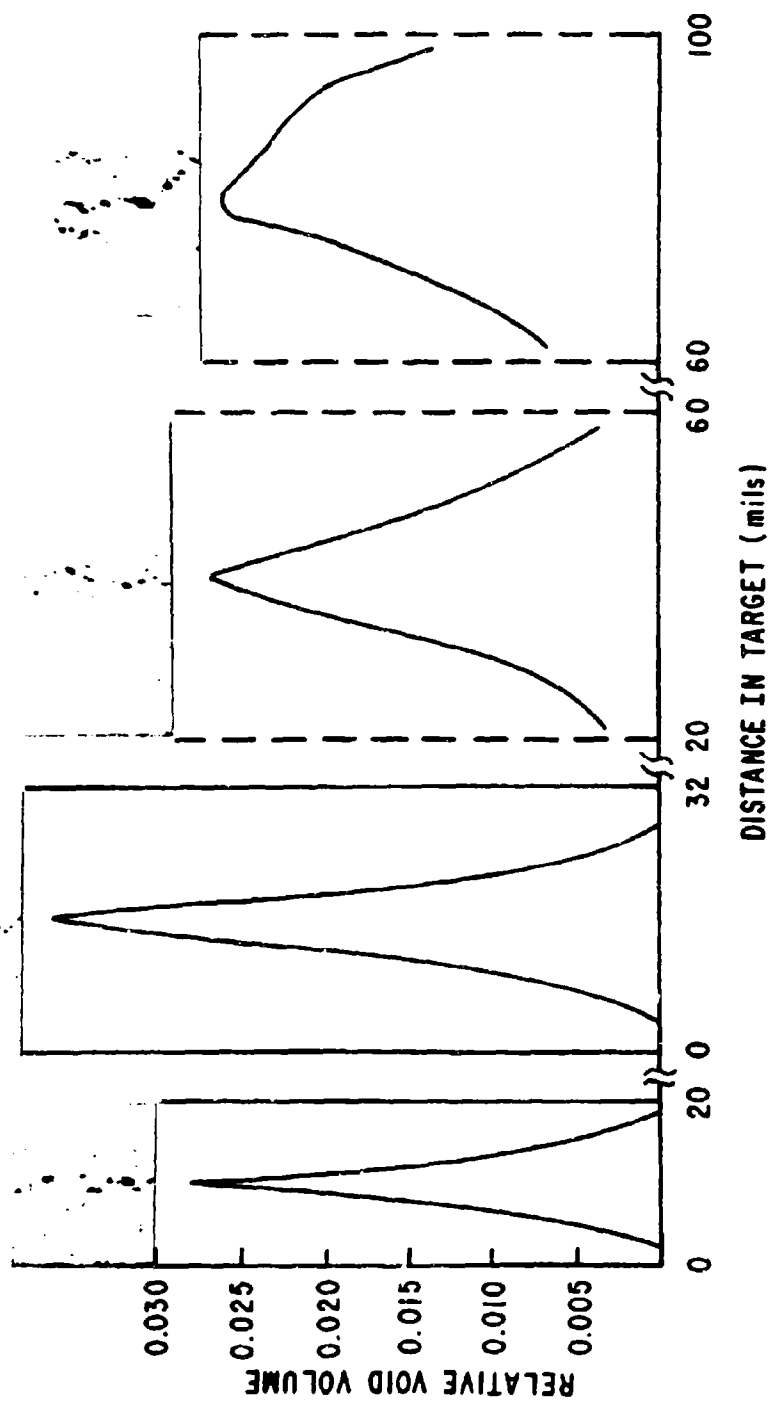
Figure 30. Damage Levels Calculated with Hole-Growth Model for AFWL Experimental Data

But perhaps the most important observation to be drawn from these comparisons is the ease with which the output from the Hole-Growth model can be interpreted. The other models considered predict inaccurate and physically unrealistic levels of damage. The Hole-Growth model provides a numerical value for the level of damage based on the relative volume of voids which can be easily correlated with photomicrographs of actual damage. Damage predictions then will provide a realistic picture of the actual material behavior.

SECTION V

CONCLUSIONS

This section summarizes the results obtained, presents the most obvious conclusions, and suggests directions for future research.

1. SUMMARY

Three separate series of impact experiments were performed on 6061-T6 aluminum targets on the AFWL 2.5 in. gas gun. The purpose of these experiments was to determine the spall threshold for the material. This data would be useful in validating various models of dynamic fracture for use in the PUFF computer code.

The first series of shots showed the time-dependency of the spall threshold but failed to bracket the threshold for the thin targets. Certain problems with the experimental configuration were indicated, and a second series of shots was planned.

The second series successfully bracketed the spall threshold. A comparison of AFWL data with that generated at other laboratories, however, revealed discrepancies, especially for short duration pulses.

To resolve these discrepancies, a third and final series of shots was planned. 6061-T6 aluminum used by General Motors to determine a spall threshold was obtained for the AFWL shots. All experimental conditions under which the AFWL data was generated were maintained so that the material was the only variable. The results of this series confirmed the GM experiments indicating that batch-to-batch variations in a "standard" commercially obtainable material may be sufficient to cause widely varying results in dynamic behavior.

Experimental results were evaluated with the use of four models of dynamic fracture: the Tuler-Butcher model, the Rate Process model, a model based on an inverse series expansion, and the Hole-Growth model developed by SRI. For data

from a single source, the Series Expansion model provided the best fit. For a large number of data points from a variety of sources, experimental scatter was severe enough that no model provided an extraordinary fit and all were acceptable.

With the models incorporated in PUFF-type computer codes, calculations were performed to determine how well the models "predicted" damage. For all but the Hole-Growth model, the results were discouraging. In addition, interpretation of the results was extremely difficult. The Hole-Growth model, however, provided easily understandable results and acceptable accuracy considering the approximations required.

2. CONCLUSIONS

There are several conclusions to be drawn from this effort. First, in the study of dynamic fracture, careful documentation of material characteristics and properties as well as interpretation of the level of damage is required. Batch-to-batch variations in the properties of "standard" 6061-T6 aluminum 'ed to a difference in spall threshold at short pulse durations of approximately 15 percent between that determined by AFWL and by General Motors. Also, while much spall data for 6061-T6 aluminum already exists, comparison of this data is made difficult by lack of complete definition of so-called "incipient" spall.

The data analysis presented in this report indicates that the Hole-Growth fracture model developed by SRI is greatly superior to other existing fracture models, both because of its accuracy and because of the ease of interpretation of calculations.

3. RECOMMENDATIONS

Because of the superiority of the SRI model, some effort should be made to acquire data sufficient to obtain the fracture parameters for at lease a minimum number of materials of interest. Proper selection of materials would provide guidelines for classes of similar materials. SRI has already used data on 1145 aluminum to predict results of experiments on copper. The predictions were within

10 percent of the results obtained. It is also recommended that some effort be exerted to extend the model to include effects of elevated temperatures.

Finally, SRI is presently extending the model to brittle failure in Armco iron and graphite. Thus, satisfactory failure criteria for homogeneous materials will be available. Some attempt should be made then to use the model for composite materials of interest. These materials represent the real problem, and no acceptable failure models exist.

This page intentionally left blank.

APPENDIX I

DETERMINATION OF CONSTANTS FROM EXPERIMENTAL DATA

The purpose of this appendix is to show the equations used to determine the necessary constants for the three empirical fracture models discussed in the text. Basically, a least-squares analysis was used. For equations of the form

$$y = y_0 + mx \tag{6}$$

best fit values for y_0 and m based upon n values of x_i and y_i are

$$y_0 = \frac{\left(\sum_{i=1}^{n} y_i\right)\left(\sum_{i=1}^{n} x_i^2\right) - \left(\sum_{i=1}^{n} x_i y_i\right)\left(\sum_{i=1}^{n} x_i\right)}{n\left(\sum_{i=1}^{n} x_i^2\right) - \left(\sum_{i=1}^{n} x_i\right)^2} \tag{7}$$

and

$$m = \frac{n\left(\sum_{i=1}^{n} x_i y_i\right) - \left(\sum_{i=1}^{n} x_i\right)\left(\sum_{i=1}^{n} y_i\right)}{n\left(\sum_{i=1}^{n} x_i^2\right) - \left(\sum_{i=1}^{n} x_i\right)^2} \tag{8}$$

The Tuler-Butcher cumulative damage failure model is

$$\int_0^t (\sigma - \sigma_0)^\lambda \, dt = K \tag{9}$$

which, for a rectangular pulse of amplitude σ and duration Δt, reduces to

$$\sigma - \sigma_0^{\lambda} \Delta t = K \tag{10}$$

Three constants are required to express $\sigma = \sigma(t)$. By assuming a value for one of these constants, the simple approach described above can be used. Thus, if a value is assumed for the exponent λ, equation (10) can be expressed as

$$\sigma = \sigma_0 + (\Delta t / K)^{-1/\lambda} \tag{11}$$

and the constants can be determined from equations (7) and (8).

Similarly, one may assume a value for σ_0. Values for the other constants may then be determined through an iterative technique which evaluate the coefficient of the Δt term for a value of λ. A standard deviation is then determined for each pair of constants in the iteration. The pair which produces the minimum standard deviation is the solution. The rate process model

$$\sigma = \sigma + A_0 \log(\Delta t) \tag{12}$$

utilizes only two constants which can be determined directly from equations (7) and (8).

The Series Expansion Model

$$\sigma = \sigma_0 + A/\Delta t + B/(\Delta t)^2 \tag{13}$$

requires evaluation of three constants. A somewhat more complex analysis was used for this model. The least-squares mdethod was used to determine all three constants. The pertinent equations are

$$T_k = \sum_{i=1}^{n} 1/\left(\Delta t_i\right)^k \quad \text{for } k = 1,2,3,4 \tag{14}$$

$$S_k = \sum_{i=1}^{n} \sigma_i/\left(\Delta t_i\right)^k \quad \text{for } k = 0,1,2 \tag{15}$$

$$\text{DENOM} = n\left(T_2 T_4 - T_3^2\right) - T_1\left(T_1 T_4 - T_2 T_3\right) + T_2\left(T_1 T_3 - T_2^2\right) \tag{16}$$

$$\sigma_0 = \frac{S_0\left(T_2 T_4 - T_3^2\right) - T_1\left(S_1 T_4 - S_2 T_3\right) + T_2\left(S_1 T_3 - S_2 T_2\right)}{\text{DENOM}} \tag{17}$$

$$A = \frac{n\left(S_1 T_4 - S_2 T_3\right) - S_0\left(T_1 T_4 - T_2 T_3\right) + T_2\left(S_2 T_1 - S_1 T_2\right)}{\text{DENOM}} \tag{18}$$

$$B = \frac{n\left(S_2 T_2 - S_1 T_3\right) - T_1\left(S_2 T_1 - S_1 T_2\right) + S_0\left(T_1 T_3 - T_2^2\right)}{\text{DENOM}} \tag{19}$$

58

APPENDIX II

INCLUSION OF FRACTURE MODELS IN P-PUFF COMPUTER CODE

Each of the fracture models discussed in the text was included in the P-PUFF computer code in order to determine how well the individual models "predicted" fracture. The original version of P-PUFF checked for fracture in the HYDRO subroutine if any zone experienced tensile (or negative) stress. The failure criterion was a critical tensile stress which, if exceeded, caused the zone to "spall".

To replace the criterion with one based on the models discussed, it is necessary to compute for each zone and each cycle some function of stress and time whose magnitude can be compared with a failure constant.

The Tuler-Butcher model for a rectangular pulse was used by determining whether or not the tensile stress in a zone exceeded the threshold stress σ_o. This is illustrated in the flowchart in figure 31. If the magnitude of the tensile stress is great enough and the zone has not already spalled, a quantity expressing cumulative damage is computed as follows:

$$K = K + \left(\sigma - \sigma_o\right)^{\lambda} * DTNH \tag{20}$$

where DTNH is the time increment for the cycle. This cumulative quantity is compared with a constant which must be exceeded for failure to occur. When failure does occur, the existing routine is used (Ref. 7).

Similarly, a cumulative quantity based on the Rate Process model can be used as a failure criterion. In this case the quantity is simply the duration of the pulse for tensile stress greater than threshold stress for each zone. The failure criterion is

$$\sigma - A * \log_{10} [DELT(J)] > \sigma_o \tag{21}$$

where DELT(J) is pulse duration for zone J. Again, the existing failure routine is used when failure occurs. Obviously though, this criterion is extremely
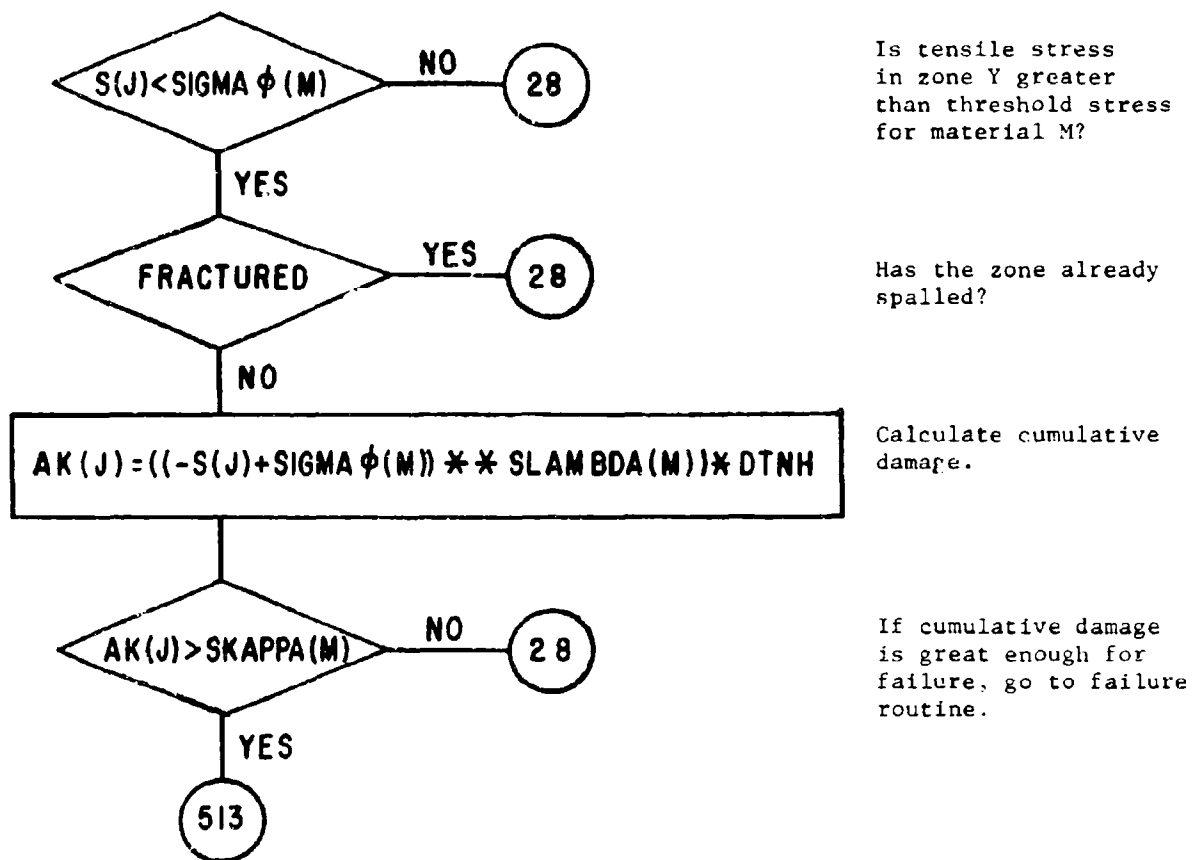
Is tensile stress
in zone Y greater
than threshold stress
for material M?

Has the zone already
spalled?

Calculate cumulative
damage.

If cumulative damage
is great enough for
failure, go to failure
routine.

Figure 31.   Flow Chart for P-PUFF Fracture Criteria

60

sensitive to pulse shape in that variations in stress amplitude severely affect the calculated results. For truly rectangular pulses, the consequences of this are minimized. However, experimental pulses are <u>not</u> truly rectangular. Thus, as a failure criteria, this model must be used with extreme caution.

The Series Expansion model also requires calculation of a quantity expressing cumulative damage. In this case

$$K = K + \left(-\sigma + \sigma_0\right) * DTNH^2 + (A * DTNH) \tag{22}$$

represents cumulative damage for each zone. This quantity is compared with B which is defined in equation (3) in the text to determine whether or not failure occurs in a zone.

The calculations based on the SRI Hole-Growth model were made with the SRIPUF4 computer code. For details concerning the fracture criterion, the reader is referred to AFWL-TR-70-99, <u>Dynamic Fracture Criteria of Homogeneous Materials</u> which provides more complete discussion than is possible here.

REFERENCES

1. Isbell, W. M., et al., <u>Measurements of Dynamic Properties of Materials</u>, DASA-2501-3, Defense Atomic Support Agency, Washington, D. C., 1970.

2. Smith, J. H., "Through Low Pressure Spall Thresholds in Copper," <u>Symposium on Dynamic Behavior of Materials</u>, ASTM, Philadelphia, 1963.

3. Jajosky, Jr., C., and Ferdman, M. A., <u>Spall Studies on 6061-T6 Aluminum</u>, AFWL-TR-69-101, Air Force Weapons Laboratory, Kirtland AFB, NM, September 1969.

4. Barbee, T. W., Seamon, L., and Crewdson, R. C., <u>Dynamic Fracture Criteria of Homogeneous Materials</u>, AFWL-TR-70-99, Air Force Weapons Laboratory, Kirtland AFB, NM, October 1970.

5. Butcher, B. M., <u>Spallation of 6061-T6 Aluminum: Behavior of Dense Media Under High Dynamic Pressure</u>, Gordon and Breach, New York, 1968.

6. Charest, J. A., Horne, D. E., and Jenrette, B. D., <u>APS Bulletin</u>, <u>14</u>, 1120, 1969.

7. Scammon, R. J., <u>The Inclusion of Fracture in the PUFF Computer Code</u>, AFWL-TR-69-73, Air Force Weapons Laboratory, Kirtland AFB, NM, July 1969.

8. Field, F. A., <u>A Simple Crack Extension Criterion for Time Dependent Spallation</u>, SAMSO-TR-69-405, Space and Missile Systems Organization, Norton AFB, CA, October 1969.

9. Breed, B. R., Mader, C. L., and Venable, D., "Technique for the Determination of Dynamic-Tensile-Strength Characteristics," <u>J. Appl Phy</u>, <u>38</u>, 3271, 1967.

10. Bru~~ck~~ ~~Superpuff Progr~~

12. Tul~~~~ and Butcher, B. M., "A Criterion for the Time-Dependence of Dynamic Fracture," <u>Int J. Fracture Mechanics</u>, 4, 431, 1968.

13. Cohen, L. J. and Berkowitz, H. M., <u>Time-Dependent Fracture Criteria for 6061-T6 Aluminum Under Stress-Wave Loading in Uniaxial Strain</u>, Douglas Paper 10191, McDonnel Douglas Astronautics Co., Huntington Beach, CA, November 1969.

14. Brodie, R. N. and Hormuth, J. E., <u>The PUFF 66 and P-PUFF 66 Computer Programs</u>, AFWL-TR-66-48, Air Force Weapons Laboratory, Kirtland AFB, NM, May 1966.

15. Kohn, B. J., <u>Compilation of Hugoniot Equations of State</u>, AFWL-TR-69-38, Air Force Weapons Laboratory, Kirtland AFB, NM, April 1969.

REFERENCES (cont'd)

16. Kruger, R. A., _A Theoretical Investigation into the Dynamic Response of Metals_, 3SR-308, Systems, Science and Software, La Jolla, CA, April 1970.

17. Berkowitz, H. M. and Cohen, L. J., _A Study of Plate-Slap Technology, Part I_, AFML-TR-69-106, Air Force Materials Laboratory, Wright-Patterson AFB, OH, May 1969.

18.

20. Butcher, B. M., Barker, L. M., Munson, D. E., and Lundergan, ʟ. D., "Influence of Stress History on Time-Dependent Spall in Metals," _AIAA_ Journal, _Volume II_, _No. 6_, June 1964.

21. Blincow, D. W. and Keller, D. V., "Experiments on the Mechanism of Spall," _Symposium_ on _Dynamic_ _Behavior_ _of_ _Materials_, ASTM, September 1962.

22. Tuler, F. R., Private Communication, Effects Technology, Inc., Santa Barbara, CA.

23. Penning, J. R., Young, D. M. and Prindle, J. H., _Negative Equation of State and Spall Criteria_, RTD-TDR-63-3039, Air Force Research and Technology Division, September 1963.

24. Dorn, J. E., Mitchell, J., and Hauser, F. E., "Dislocation Dynamics," _Exper. Mech._, _Volume V_, 1965.

This page intentionally left blank.

DOCUMENT CONTROL DATA - R & D

(Security classification of title, body of abstract and indexing annotation must be entered when the overall report is classified)

1. ORIGINATING ACTIVITY (Corporate author)	2a. REPORT SECURITY CLASSIFICATION
Air Force Weapons Laboratory (SRR) Kirtland Air Force Base, New Mexico 87117	UNCLASSIFIED
	2b. GROUP

3. REPORT TITLE

DYNAMIC FRACTURE IN 6061-T6 ALUMINUM

4. DESCRIPTIVE NOTES (Type of report and inclusive dates)

June 1969 through October 1970

5. AUTHOR(S) (First name, middle initial, last name)

James R. Kreer, Captain, USAF

6. REPORT DATE	7a. TOTAL NO. OF PAGES	7b. NO. OF REFS
January 1971	72	24

8a. CONTRACT OR GRANT NO.	9a. ORIGINATOR'S REPORT NUMBER(S)
b. PROJECT NO. 5710	AFWL-TR-70-180
c.	9b. OTHER REPORT NO(S) (Any other numbers that may be assigned this report)
d.	

10. DISTRIBUTION STATEMENT   Each transmittal of this document outside the agencies of the U. S. Government must have prior approval of AFWL (SRR), Kirtland AFB, NM 87117. Distribution is limited because of the technology discussed in the report.

11. SUPPLEMENTARY NOTES	12. SPONSORING MILITARY ACTIVITY
	AFWL (SRR) Kirtland AFB, NM 87117

13. ABSTRACT

(Distribution Limitation Statement No. 3)

Gas gun impact experiments were performed on five thicknesses of 6061-T6 aluminum targets to determine the incipient spall threshold. Data obtained were compared with previous data for the same material obtained by General Motors and other laboratories. Results indicated that batch-to-batch variations in properties of a commercially "standard" material may cause up to 15 percent differences in spall thresholds for short duration (<0.1 μ second) shock loads. Four mathematical models of dynamic fracture were evaluated with the spall data obtained. The Hole-Growth model developed by Stanford Research Institute under contract to the Air Force Weapons Laboratory proved superior to the other models considered. This superiority was manifested in the ease of interpretation of the calculated damage levels and the physical significance of the calculations.

DD FORM **1473** NOV 65   REPLACES DD FORM 1473, 1 JAN 64, WHICH IS OBSOLETE FOR ARMY USE.

14. KEY WORDS	LINK A		LINK B		LINK C	
	ROLE	WT	ROLE	WT	ROLE	WT
Dynamic fracture						
Spallation						
Fracture Modeling						